C.P. No. 658

C.P. No. 658

MINISTRY OF AVIATION

AERONAUTICAL RESEARCH COUNCIL

CURRENT PAPERS

Proving Tests of a Wingtip Parachute Installation on a Venom Aircraft, with some Measurements of Directional Stability and Rudder Power

by

F. W. Dee, A.F.R.Ae.S.

LONDON: HER MAJESTY'S STATIONERY OFFICE

1963

PRICE 7s 6d NET

U.D.C. No. A.I(42) D.H.Venom N.F.3 : 533.666.2
533.6.013.415/417

C.P. No.658
June, 1962

PROVING TESTS OF A WINGTIP PARACHUTE INSTALLATION ON A VENOM AIRCRAFT, WITH SOME MEASUREMENTS OF DIRECTIONAL STABILITY AND RUDDER POWER

by

F. W. Dee, A.F.R.Ae.S.

SUMMARY

A trial installation of a wingtip parachute has been made on a De Havilland Venom N.F.3 aircraft to check its safety and performance before use on the Fairey Delta 2. The opportunity was also taken to measure the rudder power and the directional stability derivative n_v, of the Venom.

The arrangements for streaming and jettisoning the parachute proved safe and satisfactory. The values of the directional stability derivative measured by the parachute method agreed well with values from Dutch roll tests, also made on this aircraft.

Replaces R.A.E. Technical Note No. Aero 2824 - A.R.C.24,280

LIST OF CONTENTS

		Page
1	INTRODUCTION	4
2	DESCRIPTION OF THE AIRCRAFT, PARACHUTE INSTALLATION AND GROUND TESTS	4
	2.1 The aircraft	4
	2.2 The wingtip parachute installation	4
	2.2.1 The parachute	5
	2.3 Blower tunnel tests of the installation	5
3	INSTRUMENTATION	6
	3.1 Aircraft instrumentation	6
	3.2 Parachute post instrumentation	6
	3.2.1 Calibration of strain gauges	6
4	TESTS MADE	7
5	ANALYSIS OF RESULTS	8
	5.1 General	8
	5.1.1 Parachute behaviour	8
	5.1.2 Correction of flight data	8
	5.2 Yawing moments applied by parachute	8
	5.3 Rudder power n_ζ	9
	5.4 Directional stability n_v	10
6	CONCLUSIONS	12
	LIST OF SYMBOLS	12
	LIST OF REFERENCES	13
	APPENDIX 1 - Drag of 18-inch diameter parachute used in present tests	15
	TABLE 1 - Leading particulars of test aircraft and parachute installation	16
	ILLUSTRATIONS - Figs.1-16	-
	DETACHABLE ABSTRACT CARDS	-

LIST OF ILLUSTRATIONS

	Fig.
General arrangement of De Havilland Venom N.F.3, showing wingtip parachute installation	1
Rear view of wingtip parachute installation	2
Explanatory sketch of installation	3

LIST OF ILLUSTRATIONS (CONTD.)

	Fig.
Typical strain gauge bridge circuit used to determine parachute loads	4
Method of calibrating strain gauges	5
Laboratory calibrations of the strain-gauge galvanometer systems	6
Typical flight records of parachute deployment V_i = 200 kt altitude 25,000'	7
Diagram illustrating notation used in deriving moments due to parachute drag	8
Yawing moment coefficient of 18-inch diameter parachutes used in tests	9
Control deflections to trim. With and without parachute	10
Variation of rudder angle to trim with C_L at zero sideslip. With and without parachute	11
Measured variation of rudder yawing moment derivative with C_L. Flaps up	12
Dutch roll oscillation period. Flaps up	13
Logarithmic decrement of Dutch roll oscillation	14
Directional stability. Variation of n_v with C_L. Flaps up	15
Measured drag of 18-inch diameter parachutes used in tests	16

1 INTRODUCTION

As a part of the general lateral stability test programme of the Fairey Delta 2, it is proposed to measure the rudder power and the static directional stability derivative, n_v, by means of a wingtip mounted parachute. This technique is thought to provide the most accurate method of measuring the aircraft's static yawing characteristics, and the results obtained will afford a useful comparison with the results already obtained by one of the more generally used dynamic methods[1].

During earlier tests on an Avro 707 aircraft, in which a wingtip parachute was used[2], difficulties were experienced in measuring, by mechanical means, the parachute load, which was found to fluctuate considerably. The trailing angle of the parachute was also hard to determine, as the parachute followed a coning motion in the wingtip trailing vortex. In addition, the mechanical reliability of the parachute jettison device was poor. The installation described in this Note was designed with a view to overcoming these difficulties.

The tests on the Fairey Delta 2 will be limited to equivalent airspeeds of up to 285 knots to keep the loads applied by the parachute to the wing within the aircraft design limitations. Two sizes of parachute have been designed and made for tests on this aircraft. The larger is 30 inches in diameter, and will produce a drag of approximately 1000 pounds at an equivalent airspeed of 285 knots. The second type, used in the present tests, is of 18 inches diameter, and designed for the same maximum speed. In order to economise in flying time on the Fairey Delta 2, development of the parachute attachment and its associated instrumentation was performed on a Venom N.F.3 aircraft. The opportunity was taken at the same time to measure the rudder power and directional stability derivative of this aircraft. In addition, a few Dutch roll oscillations were made to compare the dynamic and static measurements of n_v.

2 DESCRIPTION OF AIRCRAFT, PARACHUTE INSTALLATION AND GROUND TESTS

2.1 The aircraft

The De Havilland Venom N.F.3 aircraft, used in the present tests, was a two seat night fighter with a single De Havilland Ghost 103 turbojet engine, (see Fig.1). Leading particulars of the aircraft are given in Table 1. The conventional rudder and elevator controls were manually operated through cable runs, but the ailerons were power-operated. The wingtip fuel tanks were not fitted for the tests.

2.2 The wingtip parachute installation

The parachute installation, shown in Figs.2 and 3, was carried on the starboard wingtip, and comprised a supporting structure attached to the wing spar, covered by a wooden fairing which contained the streaming and jettison mechanisms.

To the supporting structure was bolted a rectangular section post, 14.75 inches in length, strain gauged to measure the forces applied to the aircraft by the parachute. The parachute was attached at the top of the post to a universal joint, consisting of a swivelling cap, and a yoke, which was free to rotate about an axis at right angles to the cap pivot. When the installation was fitted to the Venom, the axis of the post was inclined at 3.45 degrees backwards from the aircraft vertical datum.

The parachute towing strop was attached to the yoke by an explosive bolt, which, when detonated, jettisoned the parachute. The shank of the bolt passed through a closely fitting steel distance tube, which terminated at the weak point on the explosive bolt, to ensure a clean break on detonation. A swivel joint on the end of the bolt allowed the parachute to rotate without twisting the rigging lines.

In the stowed position, the parachute pack was secured on a platform at the base of the post by two bungee cords, one end of the cords being restrained by a solenoid operated bomb-release slip. On operating the slip in flight, the pack was released and was drawn off the platform by aerodynamic loads, which also deployed the parachute from the pack. The pack then fell clear of the aircraft. In the event of the pack becoming detached accidentally from the aircraft before the slip was operated, an automatic jettison device, incorporated in the fairing block, fired the bolt as soon as the pack dropped clear of the aircraft.

2.2.1 The parachute

The parachutes used for the tests were designed by Messrs. Irving Airchute Ltd., to a specification which called for an 18 inch diameter parachute which could be used at a Mach number of 1.0 at 40,000 feet altitude (an equivalent airspeed of 285 knots). This requirement was made to permit their eventual use on the Fairey Delta 2, at speeds up to a Mach number of 1.0. It will then be necessary to fly at high altitude, in order to restrict the parachute loads for reasons of wing stressing. A $2\frac{1}{2}$ foot diameter parachute, producing a drag of approximately 1000 pounds at an equivalent airspeed of 285 knots has also been made, but was not used during the present tests. The parachute canopy was of the "shaped gore" type[3], the fabric porosity being 33 cubic feet per square foot per second. The flying diameter was 18 inches. The towing strop of 1" inch single thickness flax webbing, was 10 feet long.

2.3 Blower tunnel tests of the installation

In order to prove the streaming and jettisoning characteristics of the parachute under simulated flight conditions, ground tests were made in the open jet blower tunnel at R.A.E. Farnborough. A 6 foot diameter nozzle was fitted to the tunnel mouth for the tests, and the aircraft was placed in the open jet of the tunnel with its starboard wingtip on the tunnel centre-line. The aircraft was rigged nose up to obtain a wing incidence of 5 degrees. The tunnel was run up to maximum speed, about 170 knots in this configuration, and the parachute was then streamed and developed satisfactorily. While streamed, the parachute oscillated in an apparently random manner, but this was attributed to the fluctuations in the jet velocity. There was no sign of a "coning" motion which subsequently appeared in the flight tests. It is thought that the relatively small jet diameter, and the proximity of the ground, made it impossible to simulate correctly true flight conditions. After the parachute had flown for a few seconds, during which high speed ciné records were made of its behaviour, the jettison switch was operated to fire the explosive bolt, and the parachute and towing strop were blown clear of the aircraft. On two occasions, however, distortion of the explosive bolt occurred and the parachute was not jettisoned. Modifications were therefore made to the explosive bolt assembly to prevent the bolt jamming in the distance tube on detonation. The automatic jettison device was also checked, and it was found that the parachute pack, when unrestrained by the bungee cords, blew clear of the aircraft at about 90 knots tunnel speed, and fired the explosive bolt. This indicated that the operation should be safe in flight since, if the parachute pack became detached inadvertently during take off, which is the most critical period, the jettison would occur well before the aircraft

reached its flying speed of about 120 knots. Before flight tests began, the streaming and jettisoning characteristics of the parachute were also checked and found to be satisfactory during several high-speed taxying runs.

3 INSTRUMENTATION

3.1 Aircraft instrumentation

The following quantities were measured;

Airspeed
Altitude
Aircraft incidence (range $\pm 10^{\circ}$)
Aircraft sideslip (range $\pm 10^{\circ}$)
Starboard rudder deflection (range $\pm 11^{\circ}$)
Starboard aileron deflection (range $\pm 10^{\circ}$)
Rate of roll (range $\pm 20^{\circ}$ per second)*.

Airspeed and altitude were recorded on standard aircraft instruments in an auto-observer, and the remaining quantities on Hussenot A.22 trace recorders. Film and trace records were synchronised by timing marks from a $\frac{1}{2}$ second contactor clock.

3.2 Parachute post instrumentation

The parachute post was rectangular in section, and one pair of British Thermostat SE/A/2 strain gauges was bonded symmetrically about the neutral axis, to each of the four faces. The arrangement of the two pairs of gauges can be seen in Fig.4 and also the method of connection to form a Wheatstone bridge circuit. The gauges on the other faces were similarly connected. The two bridges were used to measure the chordwise and spanwise deflections produced in the post by the parachute loads.

The out-of-balance currents in the bridge circuits resulting from loading the post were detected by two critically damped S.F.I.M. E.312 galvonometers in a Hussenot A.22 recorder. The bridges were balanced before flight by adjusting the two 2 ohm spiral-wound variable resistors connected across one output arm of each bridge. The strain gauges were energised by four 1.5 volt silver-zinc accumulators in series, the supply voltage being recorded continuously with the bridge outputs.

The parachute cable angle relative to the post was measured by a potentiometer pick-off operated by a cam on the cable attachment yoke, the output signal being recorded on an E.521 ratiometer.

3.2.1 Calibration of strain gauges

In view of the difficulty of applying pure chordwise and sidewise loads to the post while in position on the aircraft, the load calibration was performed before installing the post on the aircraft.

The calibration of the strain gauge circuits was performed with three aims:-

---

* Rate of roll was only measured during Dutch roll oscillations.

(i) to determine the sensitivity of the bridge circuits to applied loads

(ii) to investigate the effects of cross loads on the bridges

(iii) to check that no hysteresis effects were present.

The post was mounted on a plate fitted with attachment points similar to those on the aircraft installation. The plate was then bolted to a structural girder so that the post was horizontal (see Fig.5(a)). Bolt holes in the plate were arranged so that the section major axis of the post could be inclined to the vertical at angles of 0, $22\frac{1}{2}$, 45, $67\frac{1}{2}$ and 90 degrees. The post was calibrated in each position by suspending known weights from the parachute strop attachment yoke and recording the strain gauge output for each increase in load. Records were also taken as weights were removed to check for hysteresis. Care was taken to keep the maximum load applied during any calibration below the elastic limit of the post. The strain gauge supply voltage was maintained at 6.0 volts during these tests. It should be noted that the calibration was performed with the actual instrumentation subsequently used in the flight tests.

When the major axis of the post's cross-section was inclined at θ degrees to the vertical and a weight W was applied, the component of the load in the chordwise direction was $W \cos \theta$, and that in the spanwise direction $W \sin \theta$ (see Fig.5(b)). Typical calibrations of the chordwise and spanwise load gauges are shown in Figs.6(a) and (b). The curves exhibit no hysteresis, and also show that the effect of variation of cross load on the gauges is negligible for the purpose of this analysis. Slight non-linearity of the chordwise load against galvanometer deflection curve is apparent, (Fig.6(a)), but this has been taken into account in the analysis of the flight results (section 5.2). The sensitivity of the bridge galvanometer combination is such that both chordwise and spanwise loads could be determined within ±3 pounds.

4 TESTS MADE

The present tests were made at an altitude of 25,000 feet, with flaps and undercarriage up, over a range of equivalent air speeds from 150 to 295 knots, corresponding to lift coefficients between 0.55 and 0.15. The aircraft took off with the parachute stowed and climbed to 25,000 feet, where the parachute was streamed at an indicated speed of 200 knots. In order to record the no-load deflection of the galvanometers measuring the parachute loads, a short recording was made immediately before streaming the parachute.

On completion of a flight, the parachute was jettisoned over the airfield, immediately before landing. The parachute was streamed and jettisoned five times during the flight tests, each time with complete success. No inadvertent streaming or premature jettisoning occurred.

Records were made of the control deflections necessary to maintain steady straight sideslip angles of approximately 0, ±2.5 and ±5.0 degrees at indicated speeds of 152, 172, 204, 257 and 295 knots, with and without the parachute.

In addition to these steady state flight tests, a few Dutch roll oscillations were recorded at 25,000 feet, over the same speed range as that used in the static tests, to allow comparison between the value of the directional stability, n_v, measured by the parachute method, and that indicated by the period of the oscillation, (see Section 5.4).

5 ANALYSIS OF RESULTS

5.1 General

5.1.1 Parachute behaviour

A typical set of records of the deployment of the parachute in flight is shown in Fig.7. Recording was started about two seconds before the parachute was streamed. Initially the chordwise and spanwise loads are zero (Figs.7(a) and 7(c)), as the parachute post is almost completely shielded from the airflow by a fairing. On streaming the parachute, the chordwise load, Fig.7(a), rises very rapidly to its steady value as the parachute develops, while the coning motion of the developed parachute causes an oscillatory variation of the spanwise load component. The initial violent fluctuation of the cable angle trace on streaming (Fig.7(b)) is due to the cable attachment yoke, which operates the pick-off, being snatched from its stowed position into alignment with the towing strop. Thereafter, the towing strop angle varies in phase with the coning frequency. Analysis of the flight records indicated that the coning frequency was about $1\frac{1}{2}$ revolutions per second at an indicated airspeed of 150 knots, rising to 3 revolutions per second at 290 knots. The maximum included coning angle measured was about 20 degrees, but no consistent variation with airspeed was found, and in fact, the coning angle varied considerably at constant airspeed. Ref.3 states that parachutes of the type used for these tests are extremely stable, and do not deviate more than one or two degrees from their mean path. It appears, therefore, that the coning motion of the parachute was due to its entrainment in the wingtip trailing vortex, and that the use of a different shape of parachute canopy in future tests, would not improve its performance in this respect.

5.1.2 Correction of flight data

The indicated airspeed and altitude were corrected for instrument and position errors, the latter correction being derived from earlier, unpublished position error measurements on the same aircraft. Corrections were applied to the indicated incidence and sideslip to take account of the upwash and sidewash due to the noseboom, fuselage and wings. These corrections were estimated from Ref.4. Aircraft weight was found by subtracting the weight of fuel used, as noted by the pilot, from the take-off all-up weight.

5.2 Yawing moments applied by the parachute

The yawing moments applied to the aircraft by the streamed parachute were calculated from the chordwise and spanwise loads measured by the strain-gauge bridges on the parachute post, and the angle of the parachute towing cable relative to the OX-OY plane, where OX is the forward body axis, and OY that perpendicular to the aircraft plane of symmetry (see Fig.8). The laboratory calibration (Section 3.2.1) had indicated that the strain-gauge bridges were sufficiently insensitive to loads applied normal to their measuring axis for the effects of such cross loads to be neglected in the analysis.

Each strain gauge galvanometer trace deflection was measured relative to the datum established immediately before the parachute was streamed. The strain gauge supply voltage was determined, and a correction factor applied to convert the trace deflections to those appropriate to the ground calibration voltage of 6.0 volts. The values of the chordwise load P_1 and spanwise load P_2, normal to the post's neutral axis, were then determined from the calibration curves. This method was adopted to eliminate the effects of zero drift, and because of the slight non-linearity in the calibrations.

To determine the yawing moment applied to the aircraft by the coning parachute, mean values of the towing strop angle and spanwise load were found for each test. The use of mean values is considered to be justified because the coning frequency was high enough to have no measurable effect on the aircraft's behaviour, and also because the chordwise load component represented about 95% of the total parachute yawing moment, the remainder being made up of components due to non-alignment of the towing strop with the aircraft stability axis.

Accordingly, the mean value of the spanwise load $\bar{P}_2$ and the mean towing strop angle $\bar{\gamma}$ were used in conjunction with the measured chordwise load P_1, to determine the mean tensile load $\bar{P}_3$ in the parachute post, from the relation

$$-\bar{P}_3 = \sqrt{P_1^2 + \bar{P}_2^2}\,\tan\bar{\gamma}\ .$$

The yawing moment N_c applied to the aircraft by the parachute, referred to the aircraft's stability axis system may now be deduced with the aid of Fig.8 and is:-

$$N_c = -P_1\cos(\alpha+\phi)\,y + P_2[z\sin(\alpha+\phi) + x\cos(\alpha+\phi)] - P_3\sin(\alpha+\phi)\,y \qquad \ldots (1)$$

where ϕ = the angle between the neutral axis of the parachute post and the OYZ plane, being, in this case, 3.45 degrees.

As mentioned in para.5.2 apparently random variations in the parachute loads occurred during the tests at a given speed. Since, however, the test results for the control deflections have been faired to provide the control deflections to trim at zero sideslip, a mean value has been taken of the parachute yawing moment, corresponding to the zero sideslip position. Using this value of N_c, the parachute yawing moment in coefficient form may be determined as:-

$$C_{n_c} = \frac{N_c}{\frac{1}{2}\rho V^2 S\,b}\ .$$

Values of the yawing moment coefficient for the three 18 inch diameter parachutes tested are shown in Fig.9.

It is shown in Appendix 1, by analysis of the parachute load measurements, that the mean parachute drag coefficient was 0.97; this value agrees well with previous tests on similar parachutes.

5.3 Rudder power n_ζ

The deflections of the starboard aileron and rudder necessary to maintain steady straight sideslips, with and without the parachute streamed, are plotted in Fig.10 for each speed. The plots of rudder deflection against sideslip are, in general, parallel straight lines with small scatter, while

the plots of aileron deflection against sideslip show some non-linearity at lift coefficients of 0.3 and 0.4. At $C_L = 0.5$, however, the considerable scatter in the aileron angles to trim with sideslip may mask a similar non-linearity. The scatter is probably due to the difficulty in determining the true aileron trim position with the parachute streamed, since the coning motion of the parachute must have resulted in the application of a small, fluctuating, rolling moment to the aircraft. The individual test points have been faired in Fig.10 to provide a definite indication of the control deflections required to trim at zero sideslip.

In steady flight at zero sideslip, with the parachute streamed, the equation of yawing moments is:-

$$n_\zeta \Delta\zeta + n_\xi \Delta\xi + C_{n_c} = 0 \qquad (2)$$

where C_{n_c} is the yawing moment coefficient due to the parachute (Section 5.2)

$\Delta\zeta$ and $\Delta\xi$ are, respectively, the changes in rudder and aileron deflections, required to trim the parachute load.

As the aileron yawing moment was not measured in the present tests, an estimate was made from the data of Ref.5, from which $n_\xi = 0.0276\ C_L$. The contribution of the yawing moment due to aileron deflection is about 10% of that due to rudder deflection.

The rudder deflections to trim at zero sideslip, with and without parachute, are shown as a function of lift coefficient in Fig.11, and the rudder power, derived from equation (2) is given in Fig.12. It will be seen that there is comparatively little scatter in the test results, and also that the rudder power n_ζ is almost constant at -0.04 over the range of the tests. The slight decrease in rudder power at high speed, ($C_L = 0.15$ corresponds to an equivalent airspeed of 285 knots) may be due to aeroelastic distortion. The slight reduction in effectiveness at low speed may be due to the fact that the increase in incidence brings the rudder surfaces down into the wake from the fuselage and wing centre section.

5.4 Directional stability n_v

The directional stability n_v was determined in two ways:-

(i) by an analysis of the straight sideslips for the aircraft with no parachute, and

(ii) by determining the period of the Dutch roll oscillation, and using an approximate relation to find n_v.

For case (i), the equation of yawing moments is:-

$$n_\zeta \zeta + n_\xi \xi + n_v \beta = 0$$

whence $n_v = n_\zeta \left(\frac{\zeta}{-\beta}\right) + n_\xi \left(\frac{\xi}{-\beta}\right)$.

The rudder power, n_ζ, was measured in the present tests. The yawing moment due to ailerons, n_ξ, was estimated from Ref.5 to be 0.0276 C_L per radian, and the slopes of aileron and rudder deflection against sideslip without parachute were derived from Fig.10.

In method (ii), some Dutch roll oscillations, resulting from rudder kicks were recorded. In order to avoid distortion of the oscillation by accidental control inputs, the pilot was asked to leave the rudder pedals free until several complete oscillations had been recorded. Comparison of the period measured in this way, with the period measured with rudder held fixed after the kick, showed negligible difference, and it is thought that the friction in the rudder control circuit was sufficient to prevent rudder movement during the oscillation. The Dutch rolls were analysed using the approximate relation:-

$$n_v = \frac{i_c}{\mu_2}\left(\frac{2\pi\, m}{P\ \rho S V}\right)^2$$

where i_c is the yawing moment of inertia coefficient $= \frac{C}{m\ s^2}$

μ_2 is the aircraft relative density $= \frac{m}{\rho S s}$

m is the aircraft mass (slugs)

P is the period of the Dutch roll oscillation (seconds)

ρ is air density (slugs/cubic foot)

S is wing area (square feet)

s is aircraft semi-span (feet)

V is aircraft true speed (feet/second).

The value of i_c was assumed to be the same as that quoted in Ref.6, when corrected for the absence of wingtip fuel tanks in the present tests. Thus $i_c = 0.126$. P was measured from the rate of roll gyro records, and is shown in Fig.13 as a function of lift coefficient. The logarithmic decrement of the oscillation was also determined, and is presented in Fig.14, again as a function of lift coefficient. In general, both the period and damping are represented by smooth curves. The values of both period and damping at a lift coefficient of 0.375 are displaced considerably from the mean curves, and it is thought that the aircraft may have suffered an external disturbance, or possibly an involuntary control movement, which affected the oscillation.

The values of n_v derived by the two methods are presented in Fig.15. It will be seen that the results are generally in good agreement. The present Dutch roll tests give values of n_v which are slightly higher than the static method, but are dependent on an estimated value of yawing inertia. The results of the Dutch roll tests of Ref.6 are also shown in Fig.15, and these confirm the values determined in the present tests.

6 CONCLUSIONS

Flight tests to prove the safety of a wingtip parachute installation, designed for use in connection with lateral stability and control tests on the Fairey Delta 2, have indicated that the arrangements for streaming, and for normal and automatic jettisoning of the parachute are safe and satisfactory. A coning motion of the parachute which occurred is attributed to its location in the wingtip vortex, and it appears unlikely that any improvement would result from changes in parachute design.

Analysis of the results of brief flight tests made on a De Havilland Venom N.F.3 aircraft, using the parachute, shows that the rudder power may be measured accurately. Measurements of the directional stability derivative n_v, by the method of steady sideslips, agree well with values from Dutch roll tests, both on the present aircraft and on another similar aircraft.

LIST OF SYMBOLS

Measurement of parachute loads (see Fig.7)

OX, OY, OZ	body datum axes
x	distance of the parachute attachment point from the plane OYZ (feet)
y	distance of the parachute attachment point from the plane OXZ (feet)
z	distance of the parachute attachment point from the plane OXY (feet)
P_1	parachute load component normal to post N/A in X-Z plane (+ve forward) (lb)
P_2	parachute load component normal to post N/A in Y-Z plane (+ve starboard) (lb)
P_3	parachute load component parallel to post N/A (+ve down) (lb)
T	parachute strop tension (lb)
N_c	yawing moment due to parachute at zero sideslip (lb ft)
$C_{n_c} = \frac{N_c}{\frac{1}{2}\rho V^2 S b}$	
γ	angle of parachute strop to plane OXY (degrees)

General

α	wing incidence (degrees)
β	aircraft sideslip (radians or degrees)
b	aircraft wing span (feet)
C	yawing moment of inertia (slugs feet^2)

LIST OF SYMBOLS (CONTD.)

i_c yawing moment of inertia coefficient $= \frac{C}{m\,s^2}$

m aircraft mass (slugs)

P period of Dutch roll oscillation (seconds)

μ_2 aircraft relative density $= \frac{m}{\rho S s}$

ρ air density (slugs/cu ft)

s aircraft semi-span (feet)

S aircraft wing area (sq feet)

V true airspeed (ft/sec)

n_ζ derivative of yawing moment with rudder deflection (per radian)

n_v derivative of yawing moment with sideslip (per radian)

n_ξ derivative of yawing moment with aileron deflection (per radian)

ζ rudder deflection from neutral (degrees or radians)

ζ_c, ζ_o rudder deflection to trim at zero sideslip, with and without parachute respectively (degrees or radians)

ξ aileron deflection from neutral (degrees or radians)

ξ_c, ξ_o aileron deflection to trim at zero sideslip, with and without parachute respectively (degrees or radians)

$\Delta\zeta$ and $\Delta\xi$ change in rudder and aileron deflection to trim with and without parachute at zero sideslip, $\Delta\zeta = \zeta_c - \zeta_o$, $\Delta\xi = \xi_c - \xi_o$ (degrees or radians)

LIST OF REFERENCES

No.	Author	Title, etc.
1	Rose, R.	Flight measurements of the Dutch roll characteristics of a 60 degree delta wing aircraft (Fairey Delta 2) at Mach numbers from 0.4 to 1.5 with stability derivatives extracted by vector analysis. A.R.C. C.P.653. March, 1961.
2	Perry, D. H. Morrall, J. Port, W. G.	Low speed flight tests on a tailless delta aircraft with wings swept back 44.5° (Avro 707B) A.R.C. 22242. April, 1960

LIST OF REFERENCES (CONTD.)

No.	Author	Title, etc.
3	Brown, W. D.	Parachutes Sir Isaac Pitman 1951.
4	Letko, W. Danforth, E. C. B.	Theoretical investigation at subsonic speeds of the flow ahead of a slender inclined parabolic arc body of revolution, and correlation with experimental data obtained at low speeds. NACA Tech. Note No. 3205 July 1954.
5	Weick, F. E. Jones, R. T.	Resumé and analysis of NACA lateral control research. NACA Report No.605 ARC 3508 1937.
6	Perry, D. H.	Flight tests of the lateral stability of the De Havilland Sea Venom, with blowing over the flaps. ARC 22055 February 1960.

APPENDIX 1

DRAG OF 18-INCH DIAMETER PARACHUTES USED IN PRESENT TESTS

The mutually perpendicular components of the parachute load P_1, $\bar{P}_2$ and $\bar{P}_3$ (Section 5.2) may be combined to give the drag of the parachute, since, by reference to Fig.8,

$$T = \sqrt{P_1^2 + \bar{P}_2^2 + \bar{P}_3^2}\,.$$

The parachute drag thus derived is shown in Fig.16 as a function of the dynamic head q, for the three parachutes tested. In this figure the results for different parachutes are shown by different symbols, and several measurements on each parachute under nominally similar conditions are included. The full line in the figure, representing the closest linear variation in drag with q which will fit the experimental points, yields a mean drag coefficient of 0.97, if a constant flying diameter of 18 inches is assumed. Closer examination of the experimental points shows, however, that the variation in parachute drag with dynamic pressure does not conform exactly to a simple linear relationship, while consistent differences may also be noted in the behaviour of the individual parachutes, although they were nominally similar in shape and construction. It is thought that both of these effects may be attributed to changes in shape and effective diameter of the inflated parachute canopies.

It will also be noted that there was an appreciable variation in the load measured for any given parachute at the same free stream dynamic pressure. This variation seemed to be a random effect, with no apparent dependence on any of the measured flight parameters. It is possible, however, that this effect was connected with the apparently random variation in the coning behaviour of the parachute mentioned previously.

TABLE 1

Leading particulars of test aircraft and parachute installation

Wing span	38.6 feet
Wing area	279 square feet
Wing incidence (rel. to fuselage datum)	0
Dihedral	3 degrees
Aileron area (each)	9.34 square feet
Aileron movement	±15 degrees
Rudder area (each)	3.05 square feet
Rudder movement	±24 degrees
All-up-weight at take-off	12910 pounds
Weight at half-fuel	10260 pounds
C.G. position at half-fuel	0.5 feet forward of aircraft datum (37.5% centre line chord)
Yawing moment of inertia coefficient (half-fuel)	0.126
Distance of parachute attachment from aircraft centre-line datum	18.56 feet
Height of parachute attachment above aircraft datum	1.95 feet
Distance of parachute attachment aft of aircraft datum	4.25 feet

W.T.59. K3. Printed in England for H.M. Stationery Office by R.A.E. Farnborough

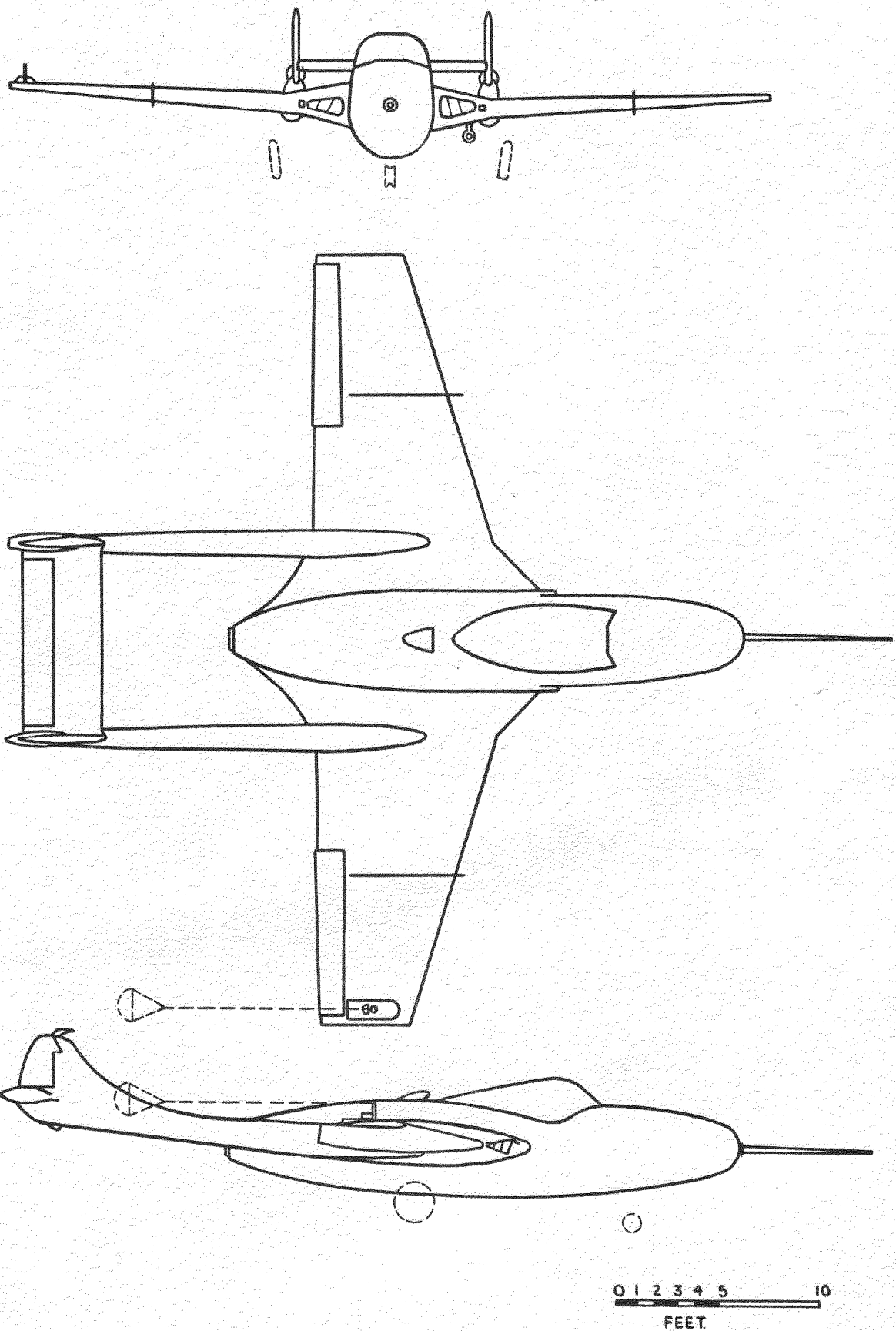

FIG I-6A OF VENOM NF3 SHOWING WINGTIP

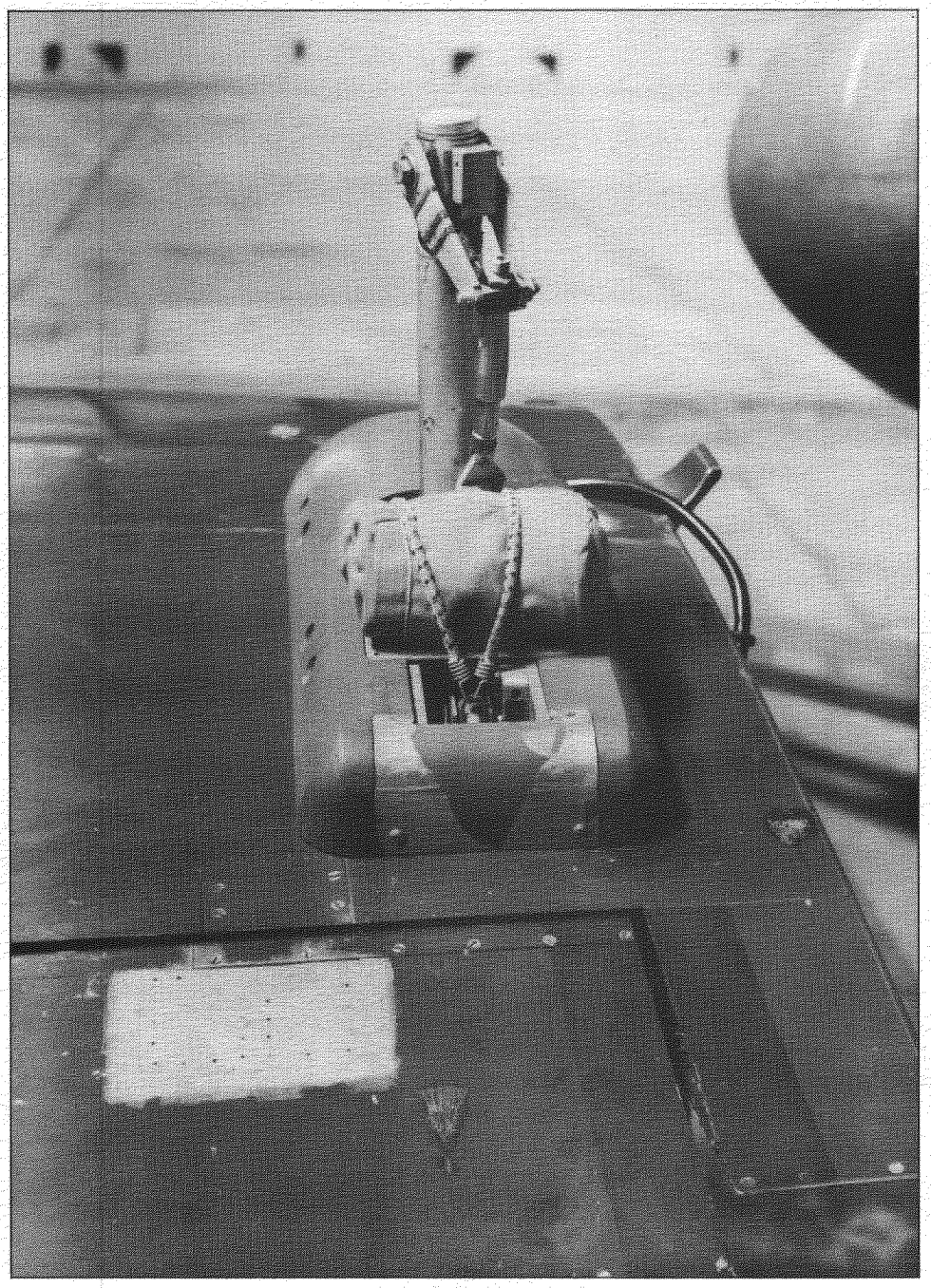

FIG.2. REAR VIEW OF WINGTIP PARACHUTE INSTALLATION

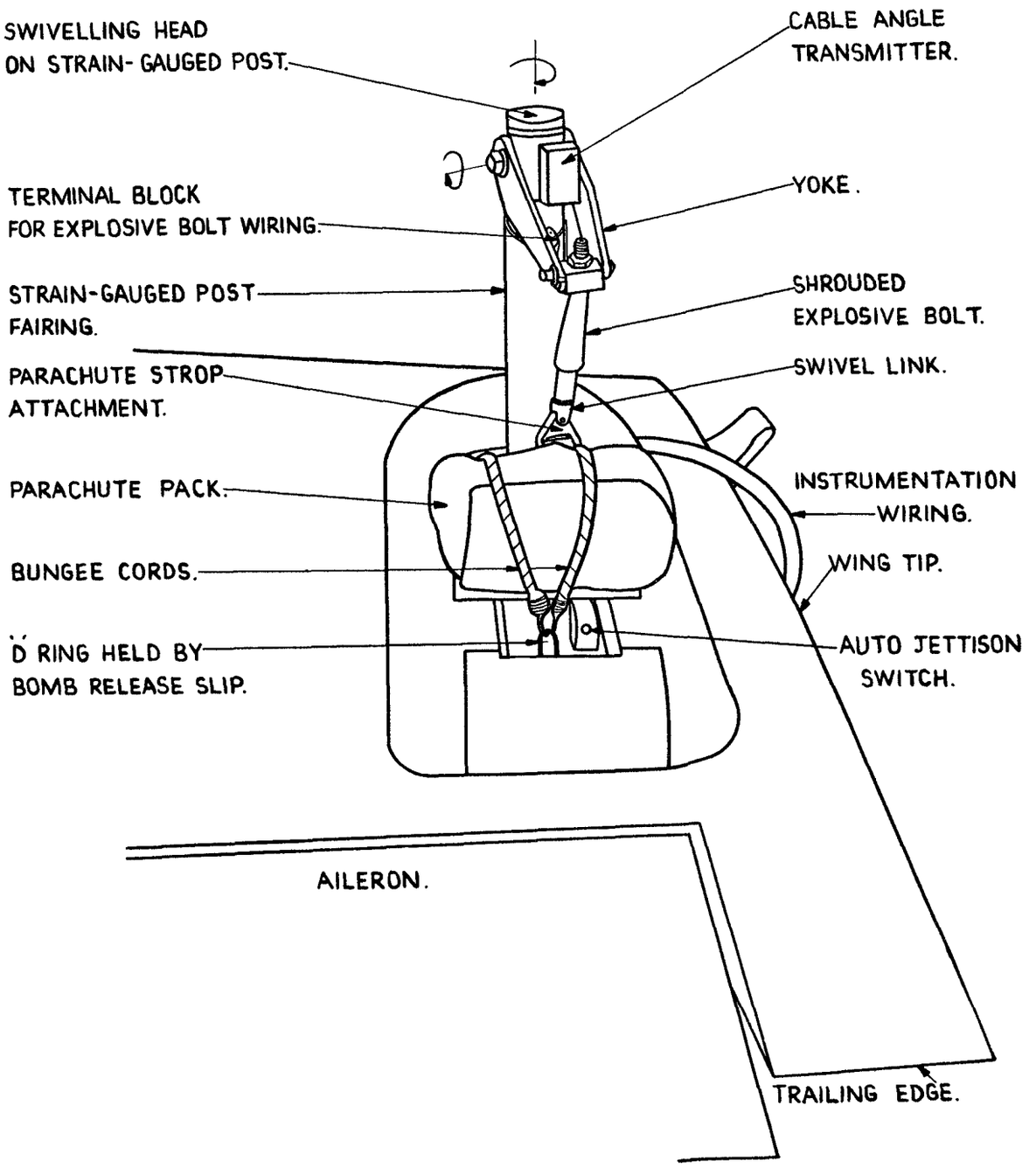

FIG.3. EXPLANATORY SKETCH OF INSTALLATION.

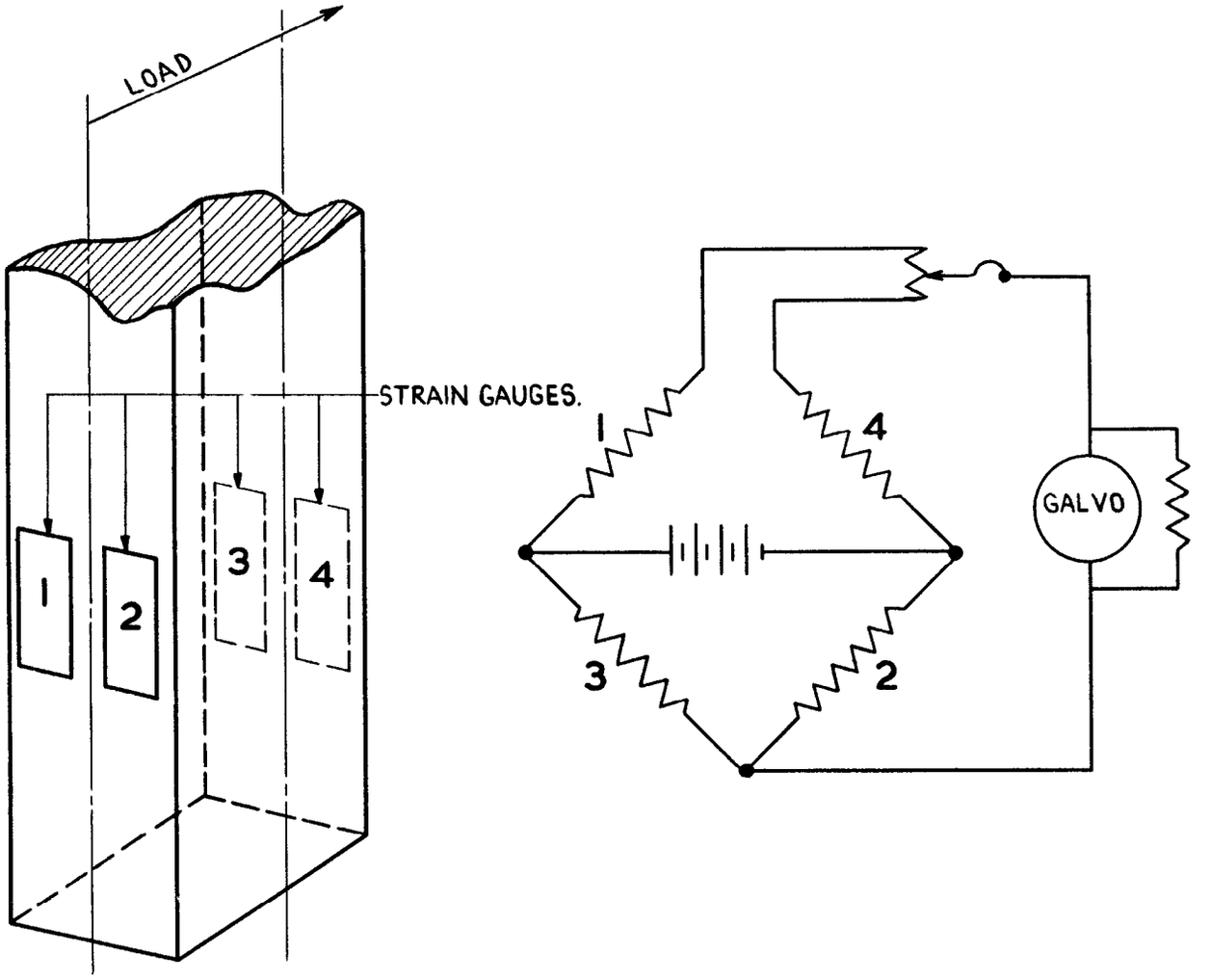

FIG. 4. TYPICAL BRIDGE CIRCUIT USED TO DETERMINE PARACHUTE LOADS.

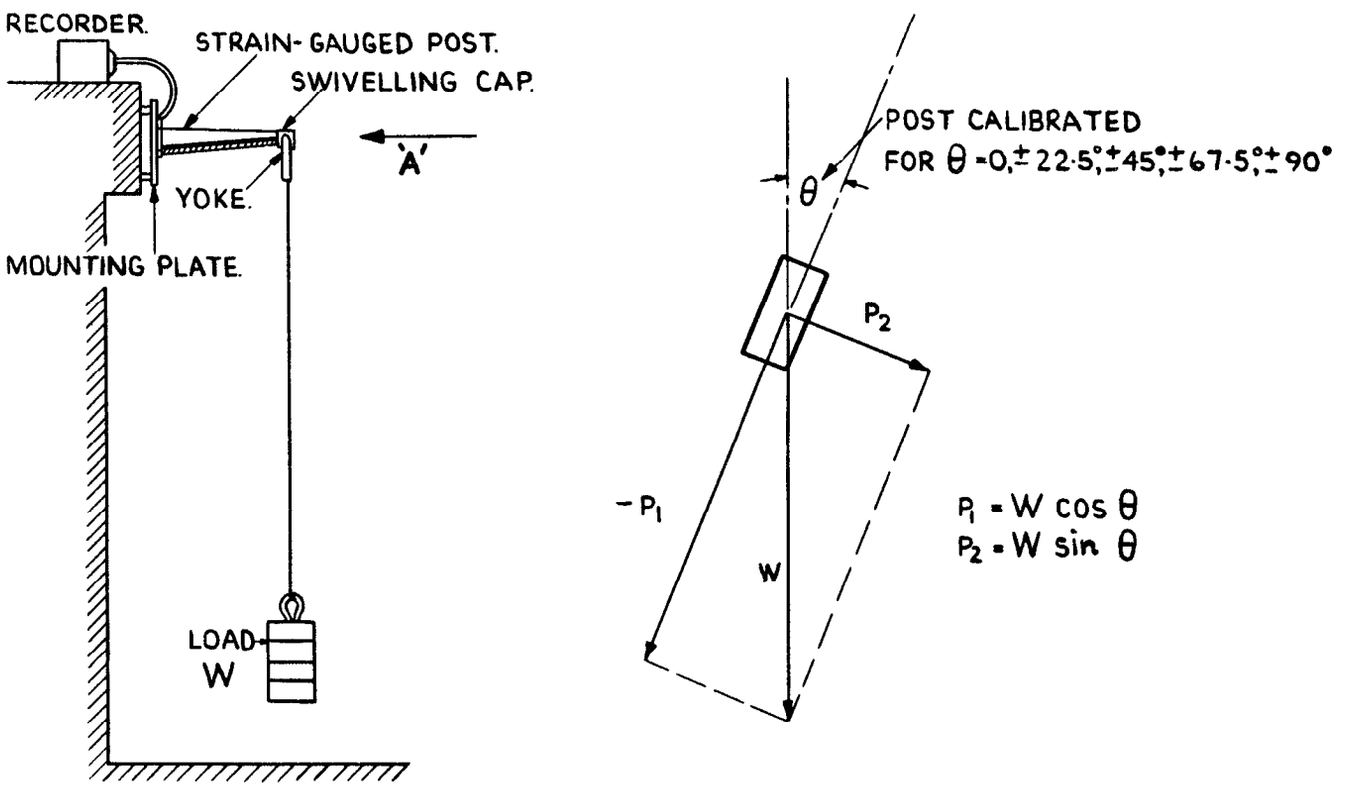

(a) SIDE VIEW OF CALIBRATION RIG. (b) DIAGRAMMATIC VIEW ON 'A'.

FIG. 5. METHOD OF CALIBRATING STRAIN GAUGES.

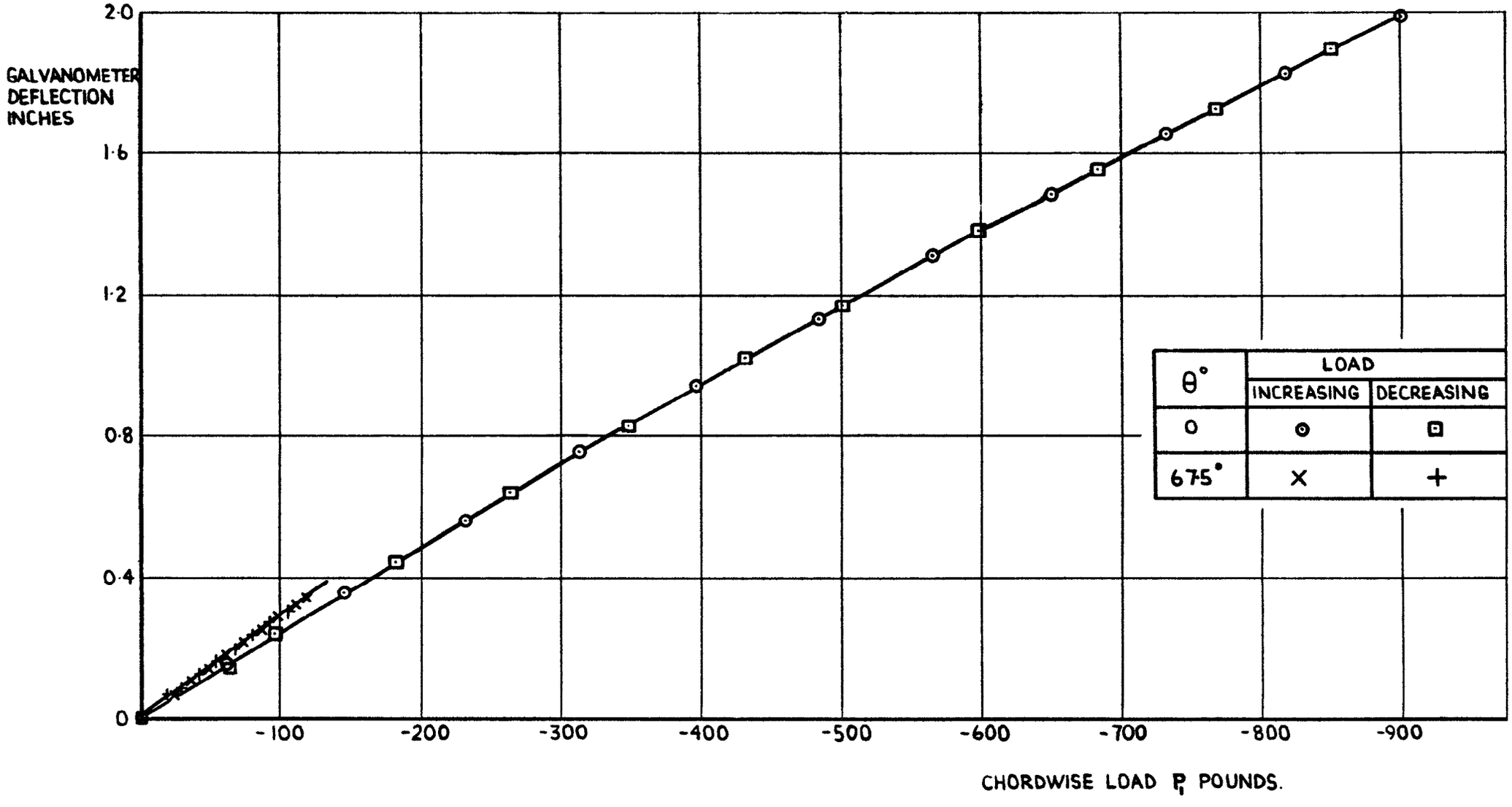

(a) CHORDWISE LOAD STRAIN-GAUGE CALIBRATION.

FIG.6. LABORATORY CALIBRATIONS OF THE STRAIN GAUGE-GALVANOMETER SYSTEMS.

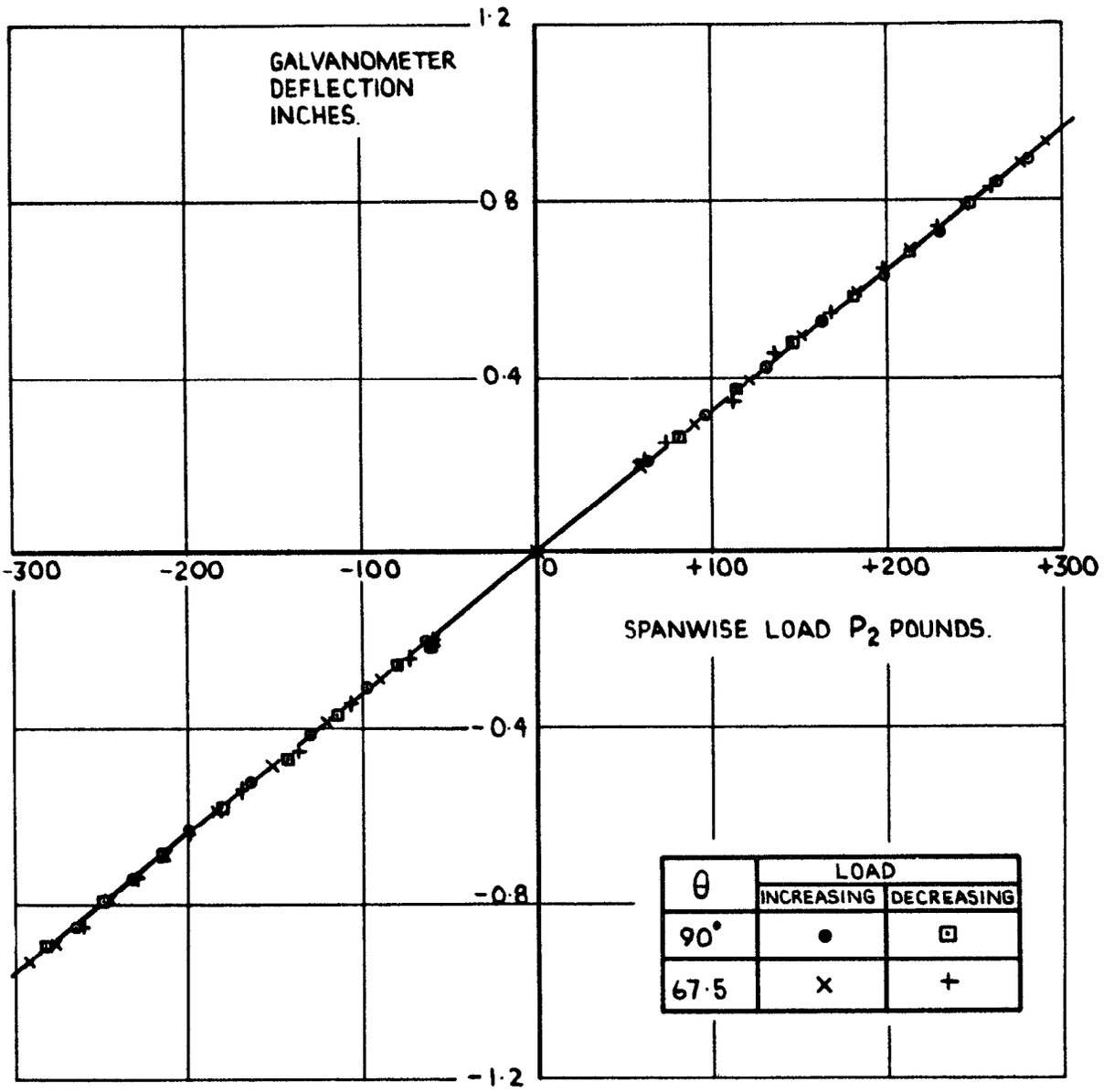

(b) SPANWISE LOAD STRAIN-GAUGE CALIBRATION.

FIG. 6. (CONT'D) LABORATORY CALIBRATIONS OF THE STRAIN GAUGE-GALVANOMETER SYSTEMS.

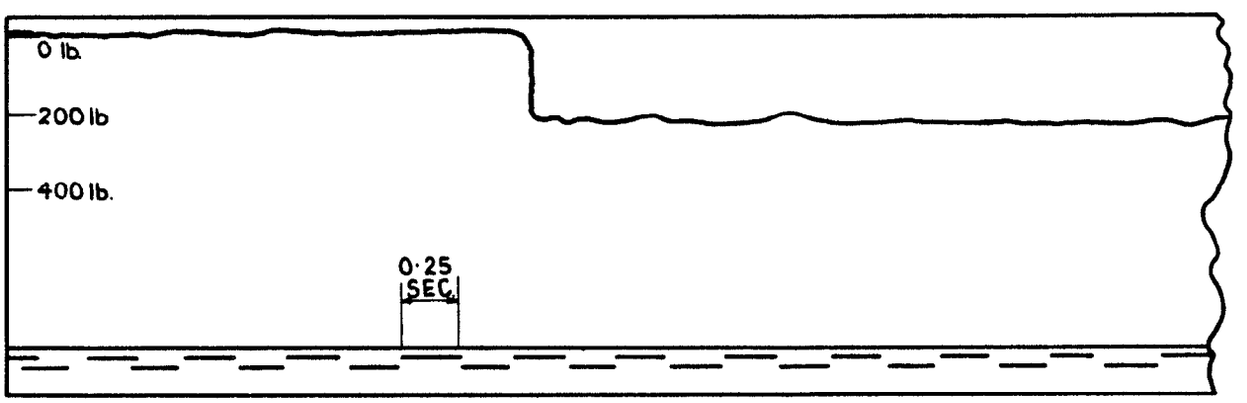

(a) PARACHUTE CHORDWISE LOAD.

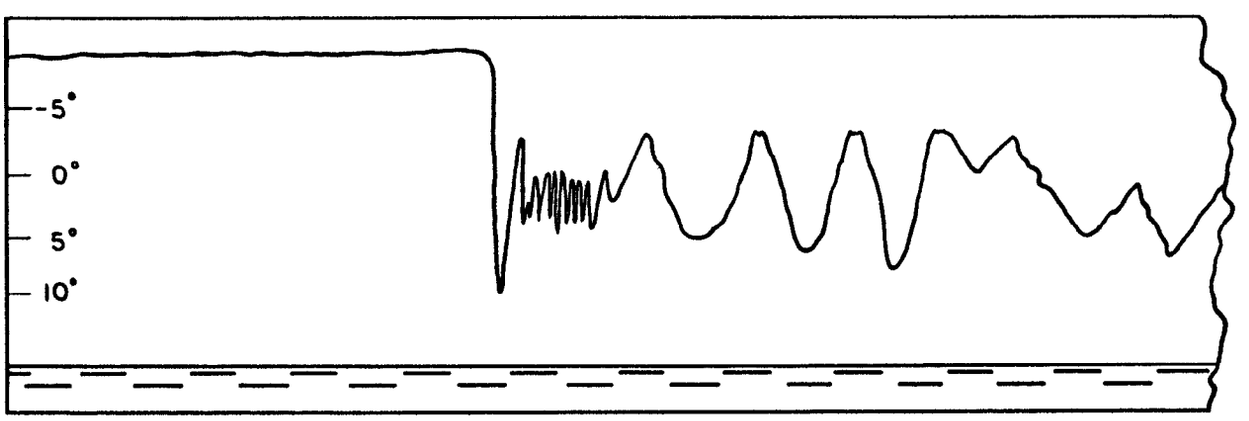

(b) PARACHUTE CABLE ANGLE. (REL TO WING CHORD)

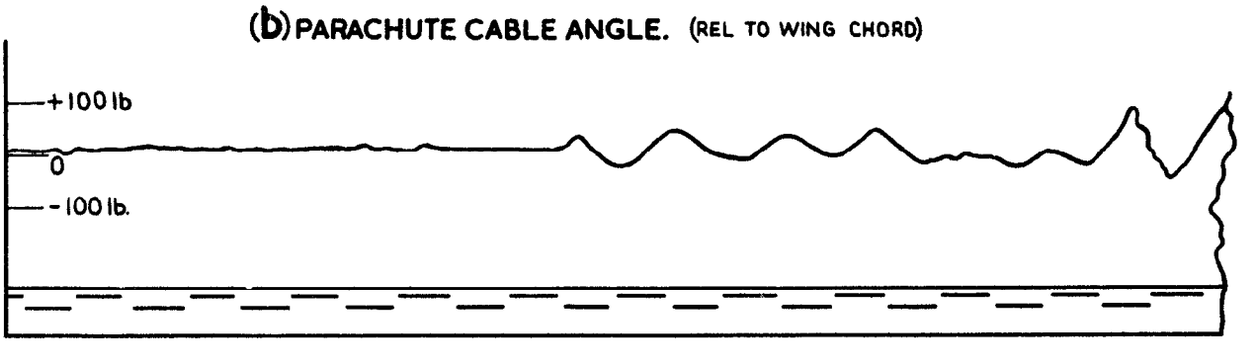

(c) PARACHUTE SPANWISE LOAD.

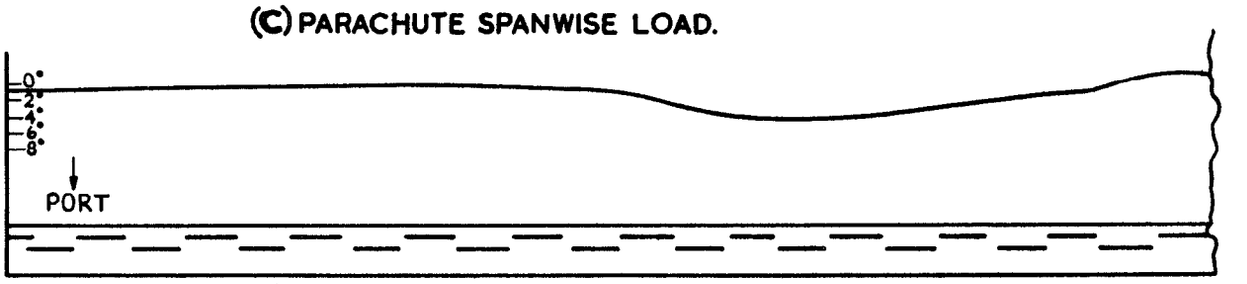

(d) AIRCRAFT SIDESLIP.

FIG. 7. TYPICAL FLIGHT RECORD OF PARACHUTE DEPLOYMENT
V_I = 200 KT. ALT. 25,000'.

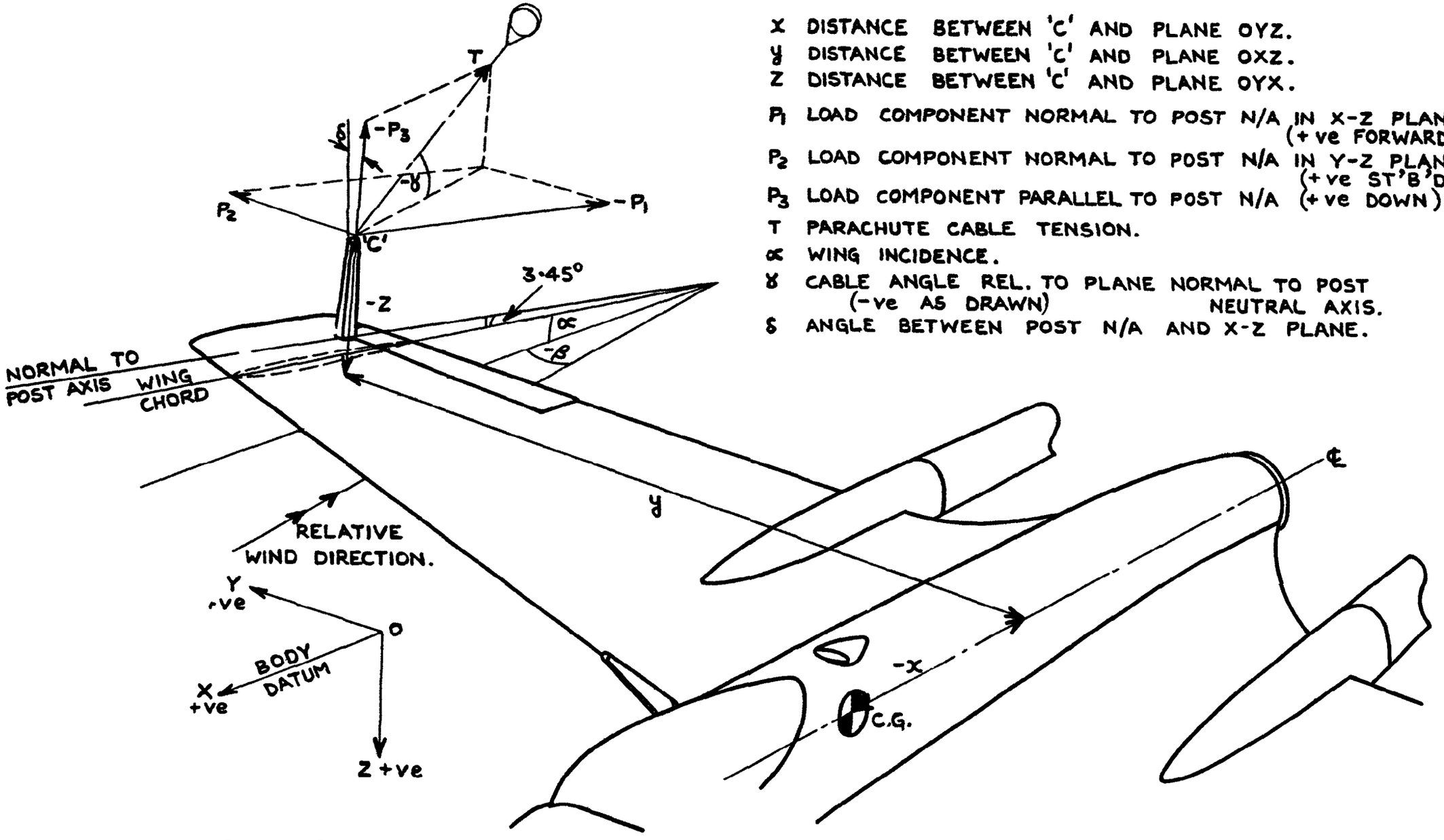

x DISTANCE BETWEEN 'C' AND PLANE OYZ.
y DISTANCE BETWEEN 'C' AND PLANE OXZ.
Z DISTANCE BETWEEN 'C' AND PLANE OYX.
P_1 LOAD COMPONENT NORMAL TO POST N/A IN X-Z PLANE (+ve FORWARD)
P_2 LOAD COMPONENT NORMAL TO POST N/A IN Y-Z PLANE (+ve ST'B'D.)
P_3 LOAD COMPONENT PARALLEL TO POST N/A (+ve DOWN)
T PARACHUTE CABLE TENSION.
α WING INCIDENCE.
γ CABLE ANGLE REL. TO PLANE NORMAL TO POST (-ve AS DRAWN) NEUTRAL AXIS.
δ ANGLE BETWEEN POST N/A AND X-Z PLANE.

FIG. 8. DIAGRAM ILLUSTRATING NOTATION USED IN DERIVING MOMENTS DUE TO PARACHUTE DRAG.

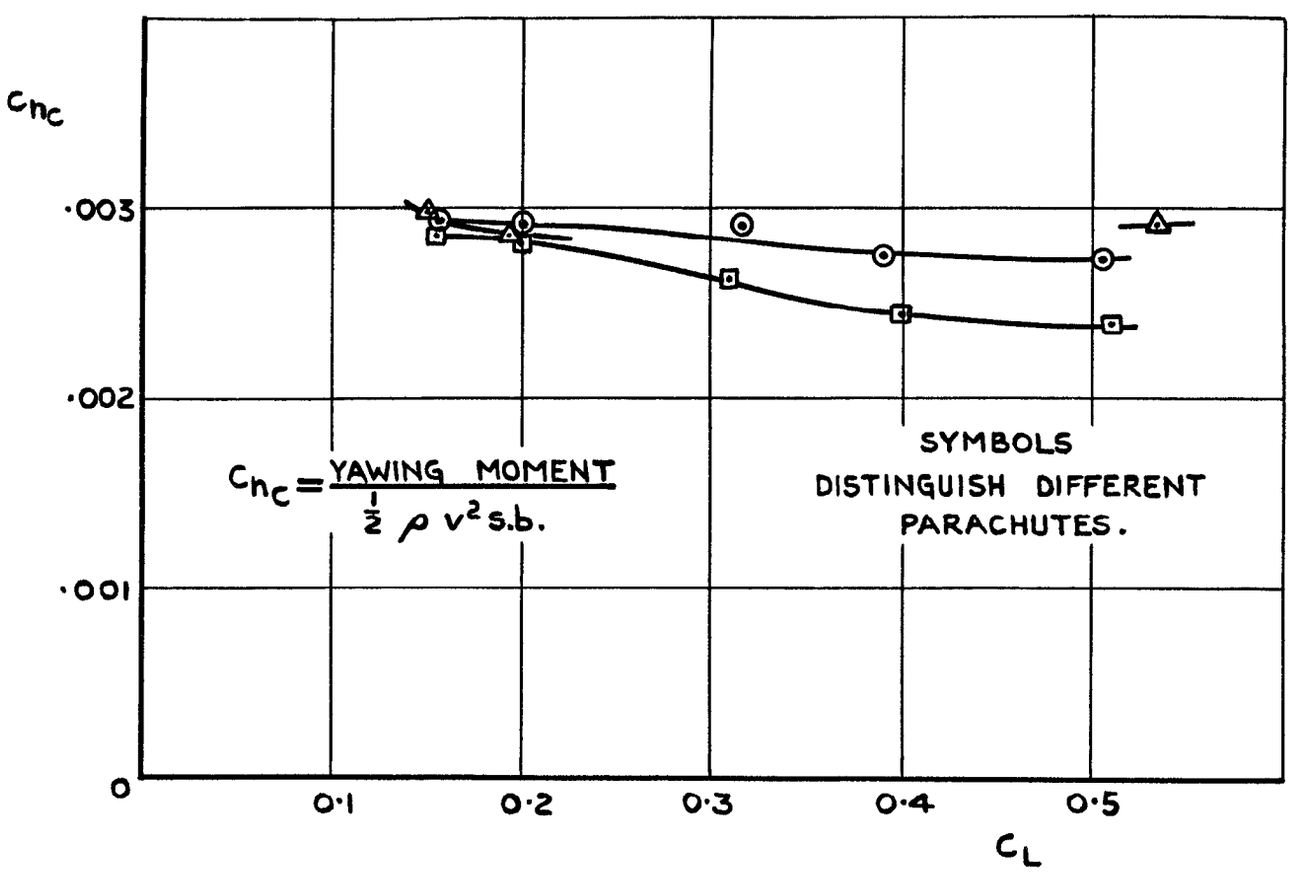

FIG. 9. YAWING MOMENT COEFFICIENT OF 18" FLYING DIAMETER PARACHUTES USED IN TESTS.

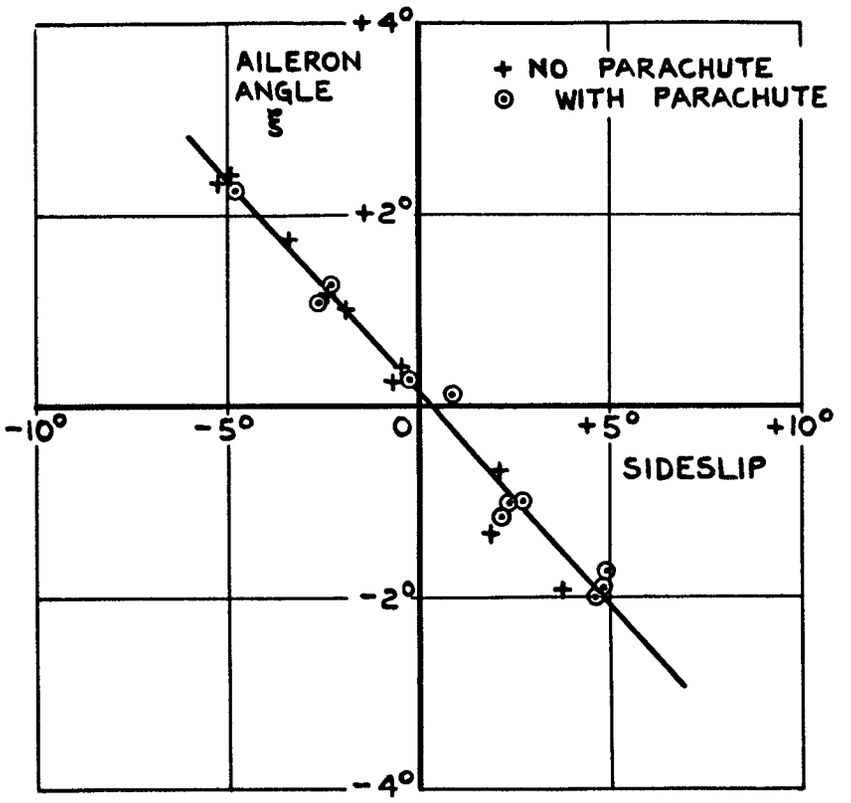

(a) AILERON ANGLE vs SIDESLIP $C_L = 0 \cdot 15$.

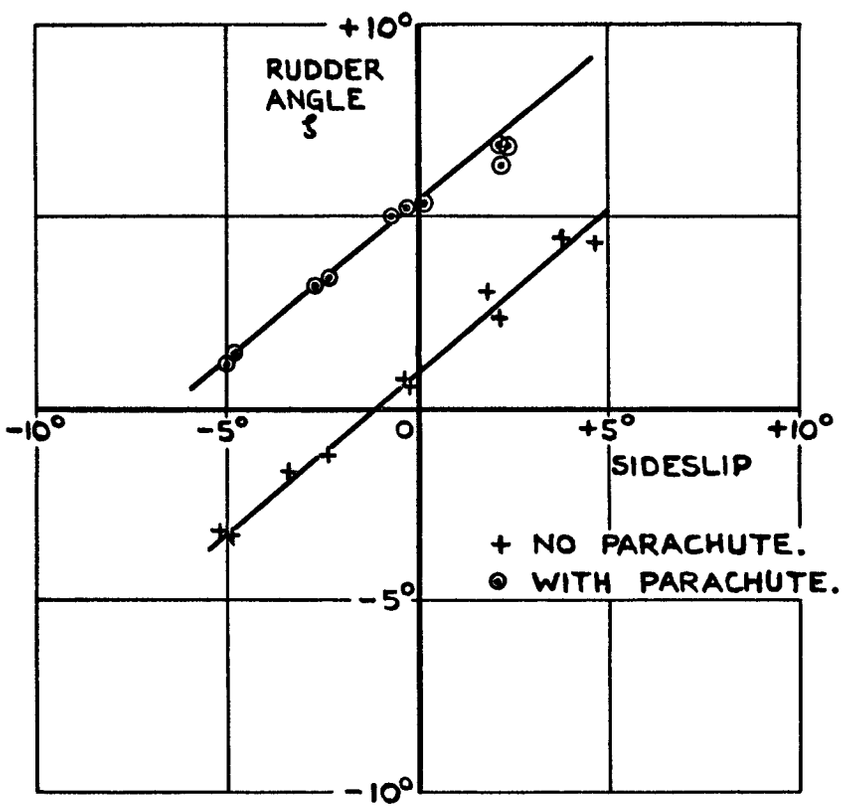

(b) RUDDER ANGLE vs SIDESLIP $C_L = 0 \cdot 15$.

FIG. 10. CONTROL DEFLECTIONS TO TRIM WITH AND WITHOUT PARACHUTE.

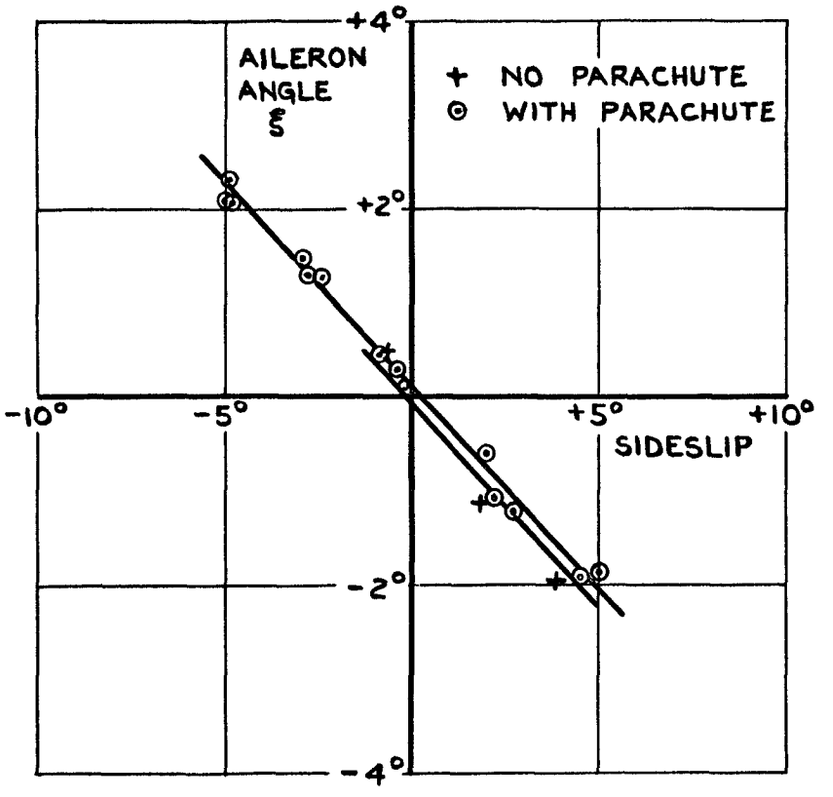

(c) AILERON ANGLE vs SIDESLIP C_L=0·20

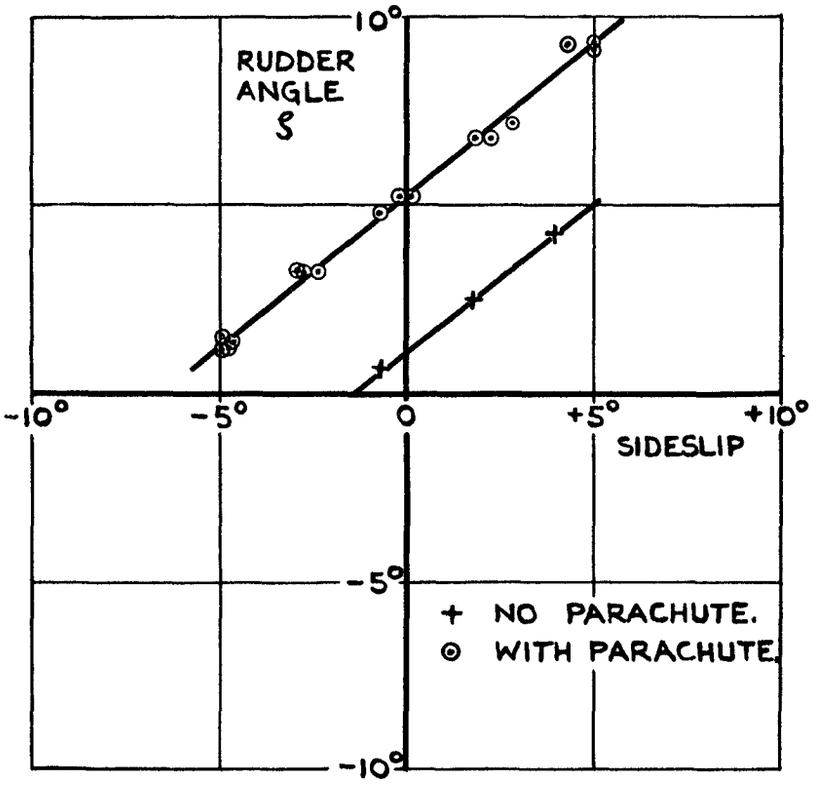

(d) RUDDER ANGLE vs SIDESLIP C_L=0·20.

FIG. 10 (CONT.) CONTROL DEFLECTIONS TO TRIM WITH AND WITHOUT PARACHUTE.

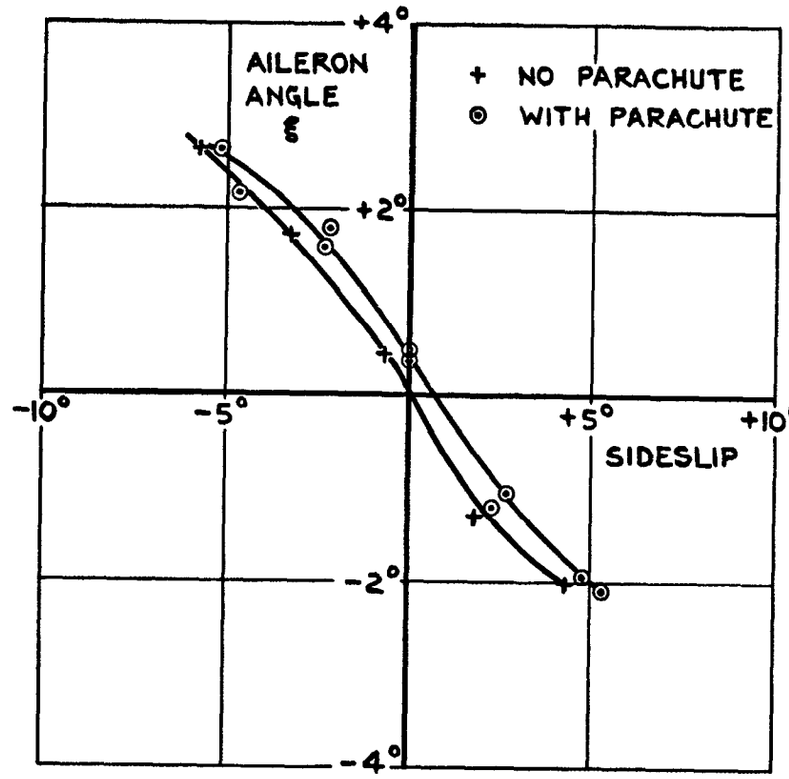

(e) AILERON ANGLE vs SIDESLIP C_L=0·31.

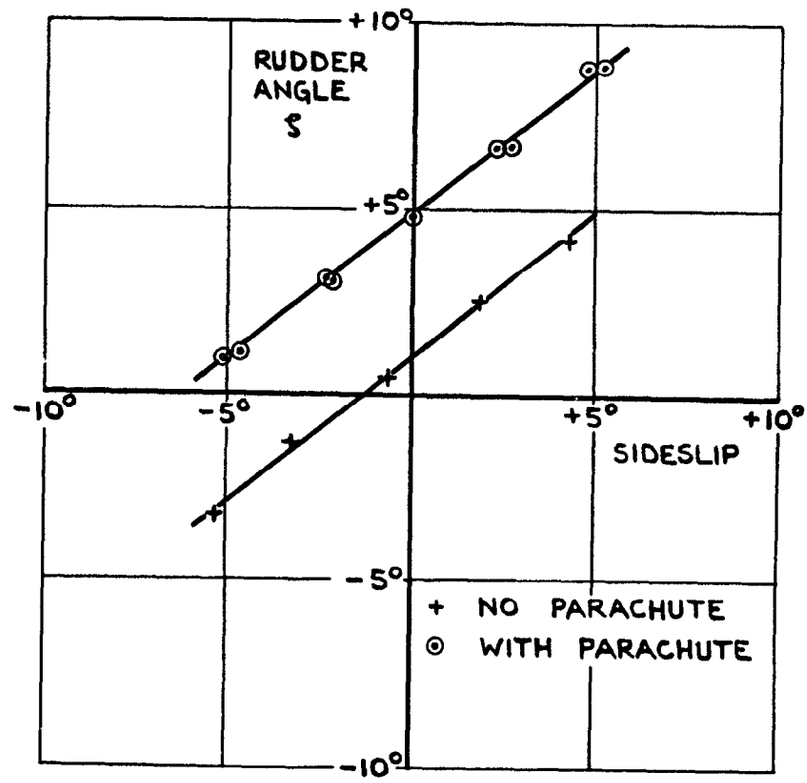

(f) RUDDER ANGLE vs SIDESLIP C_L=0·31.

FIG. 10 (CONT.) CONTROL DEFLECTIONS TO TRIM WITH AND WITHOUT PARACHUTE.

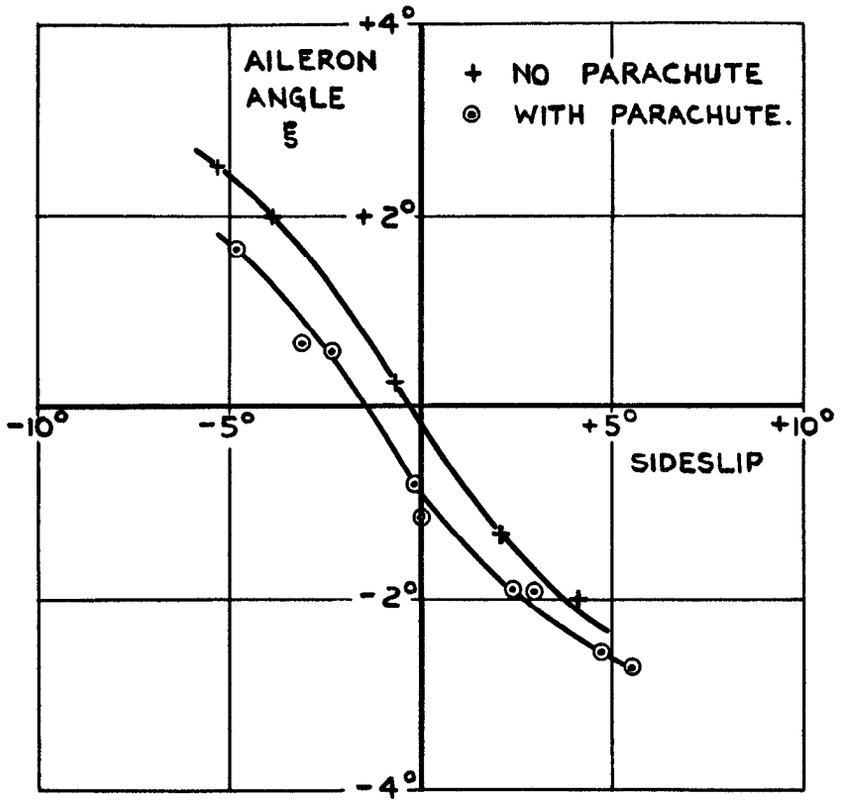

(g) AILERON ANGLE vs SIDESLIP $C_L = 0{\cdot}40$.

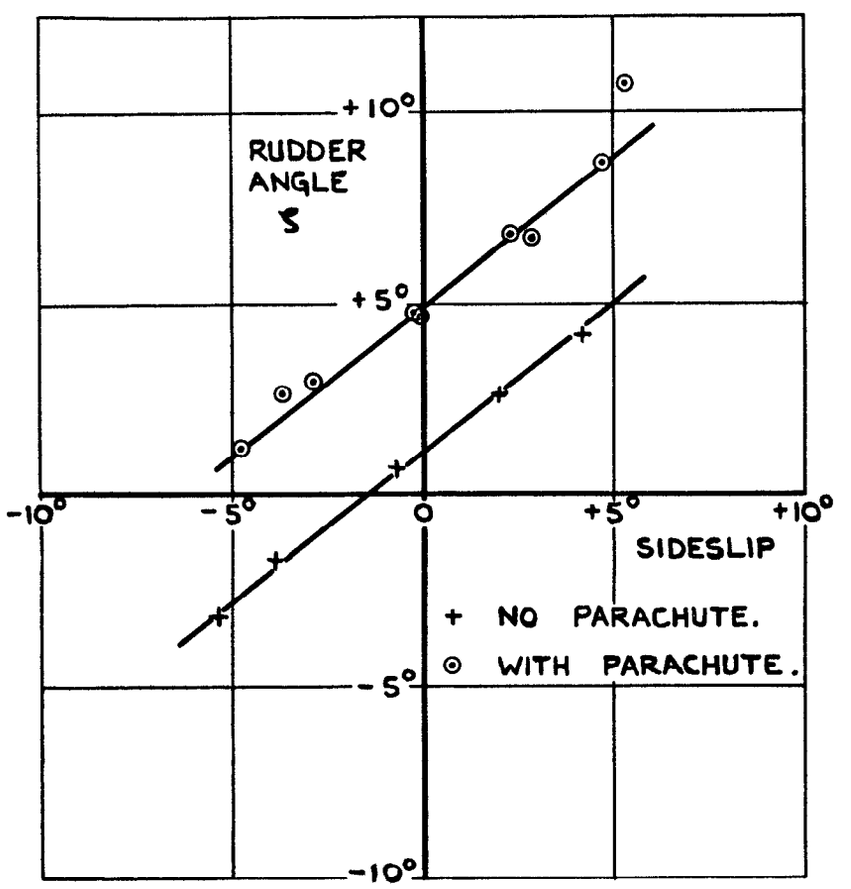

(h) RUDDER ANGLE vs SIDESLIP $C_L = 0{\cdot}40$.

FIG. 10. (CONT.) CONTROL DEFLECTIONS TO TRIM WITH AND WITHOUT PARACHUTE.

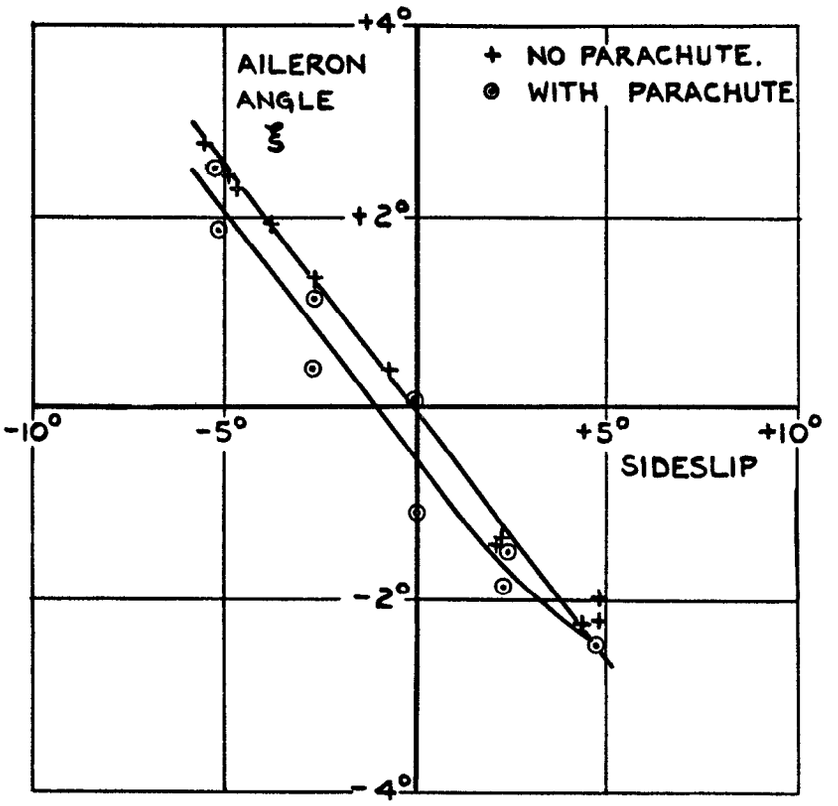

(I) AILERON ANGLE vs SIDESLIP $C_L = 0{\cdot}52$.

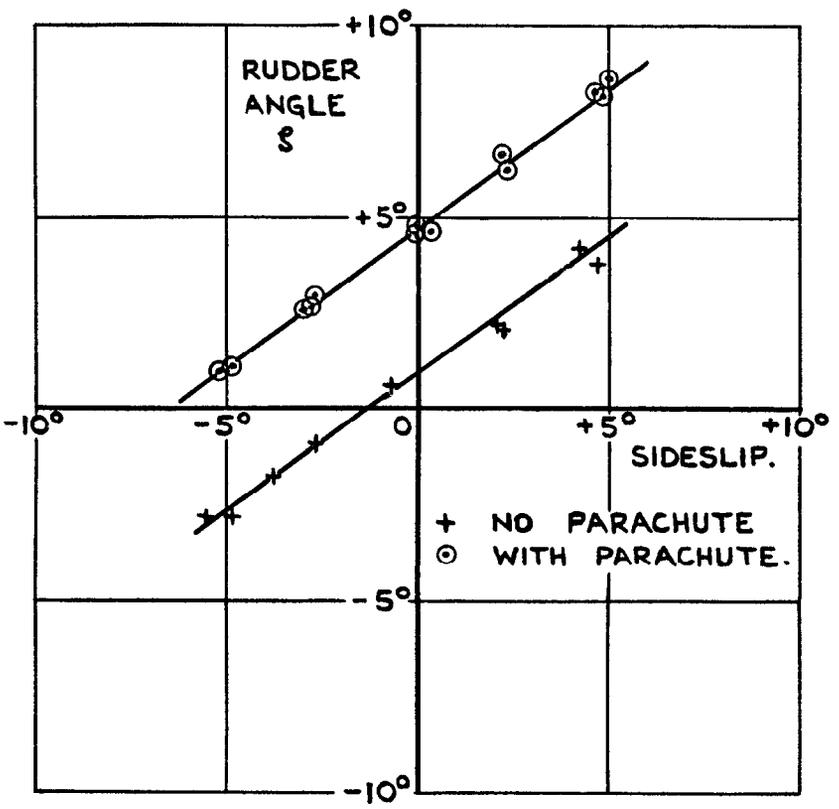

(J) RUDDER ANGLE vs SIDESLIP $C_L = 0{\cdot}52$.

FIG. 10. (CONCLD) CONTROL DEFLECTIONS TO TRIM WITH AND WITHOUT PARACHUTE.

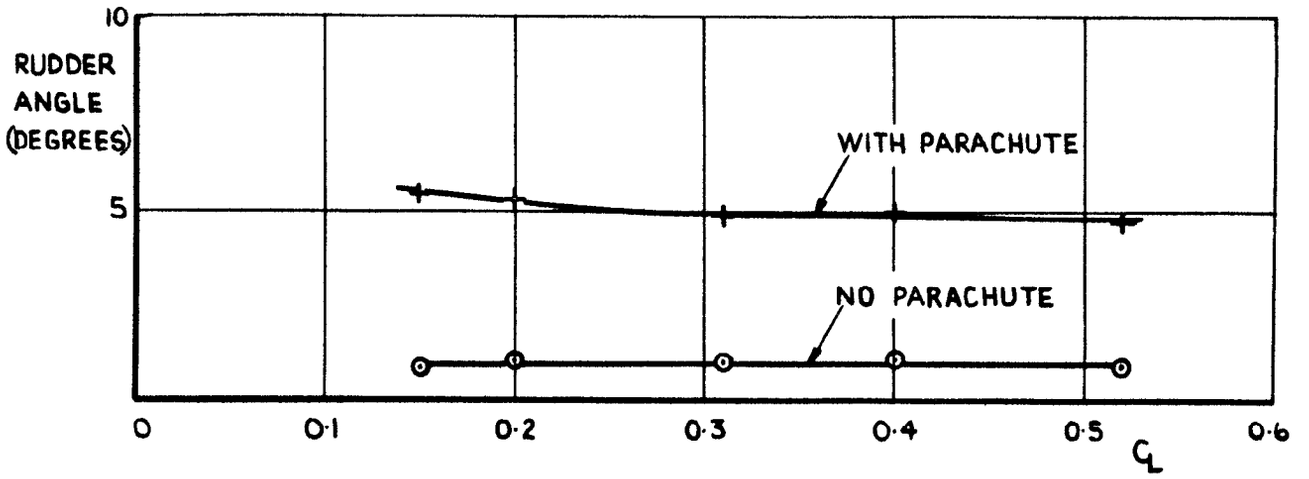

FIG. 11. VARIATION OF RUDDER ANGLE TO TRIM WITH C_L AT ZERO SIDESLIP. WITH AND WITHOUT PARACHUTE.

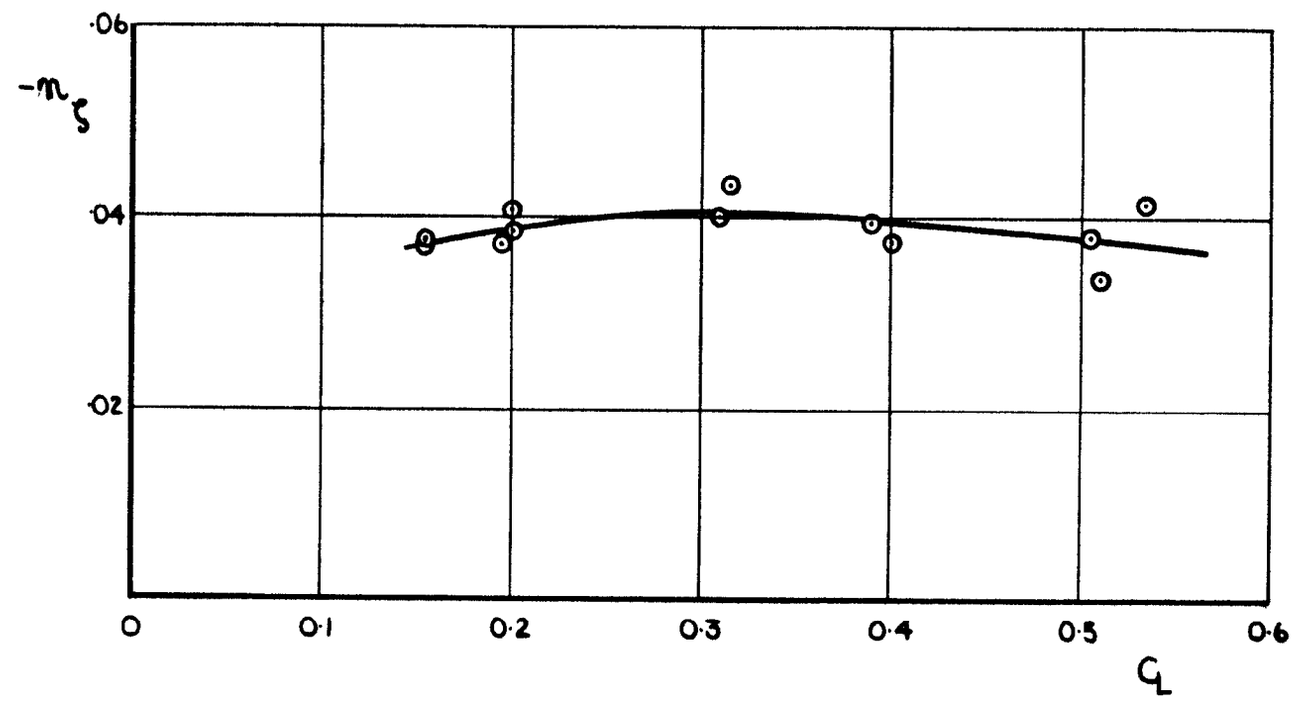

FIG. 12. MEASURED VARIATION OF RUDDER YAWING MOMENT DERIVATIVE WITH C_L. FLAPS UP.

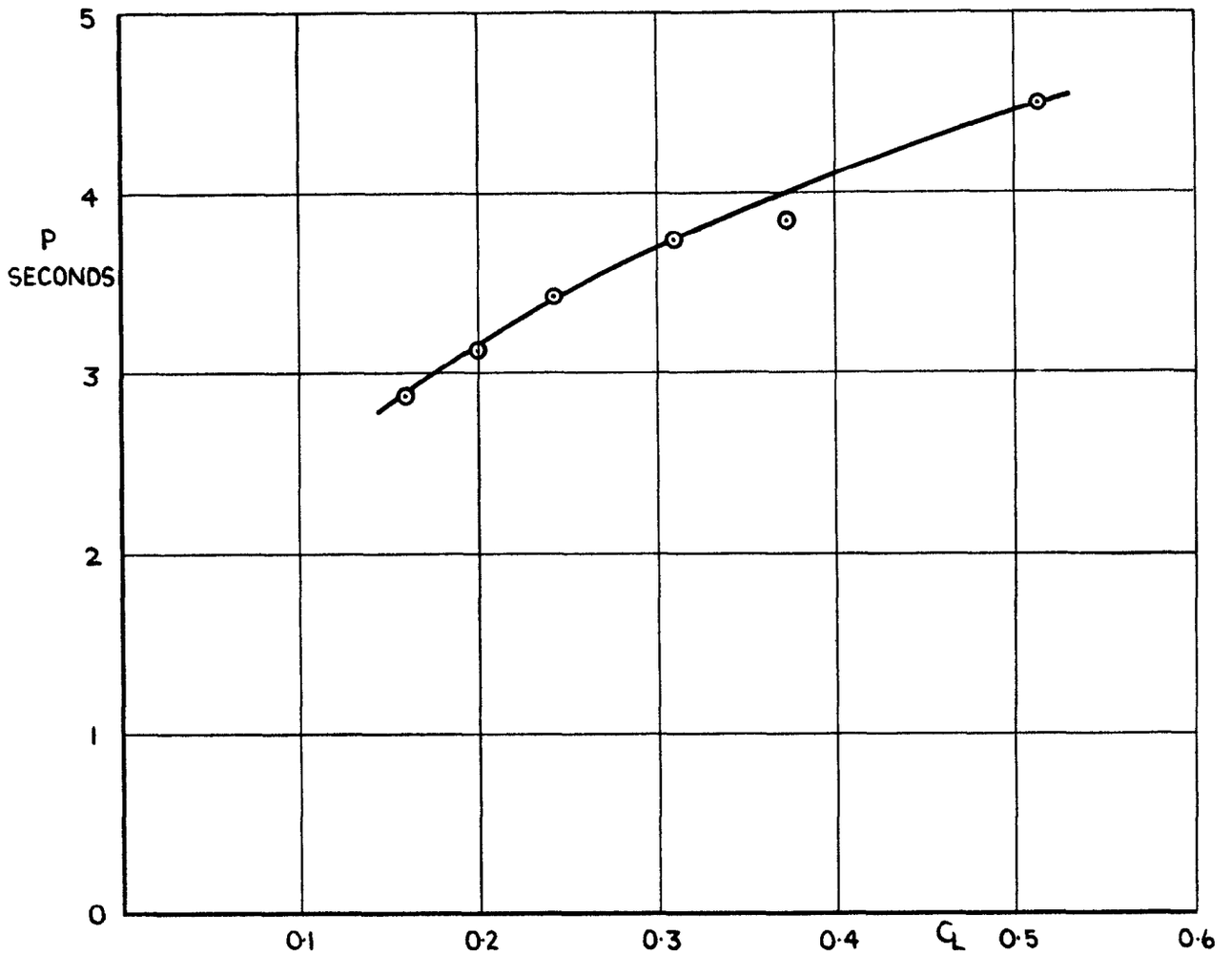

FIG. 13. DUTCH ROLL OSCILLATION PERIOD. FLAPS UP.

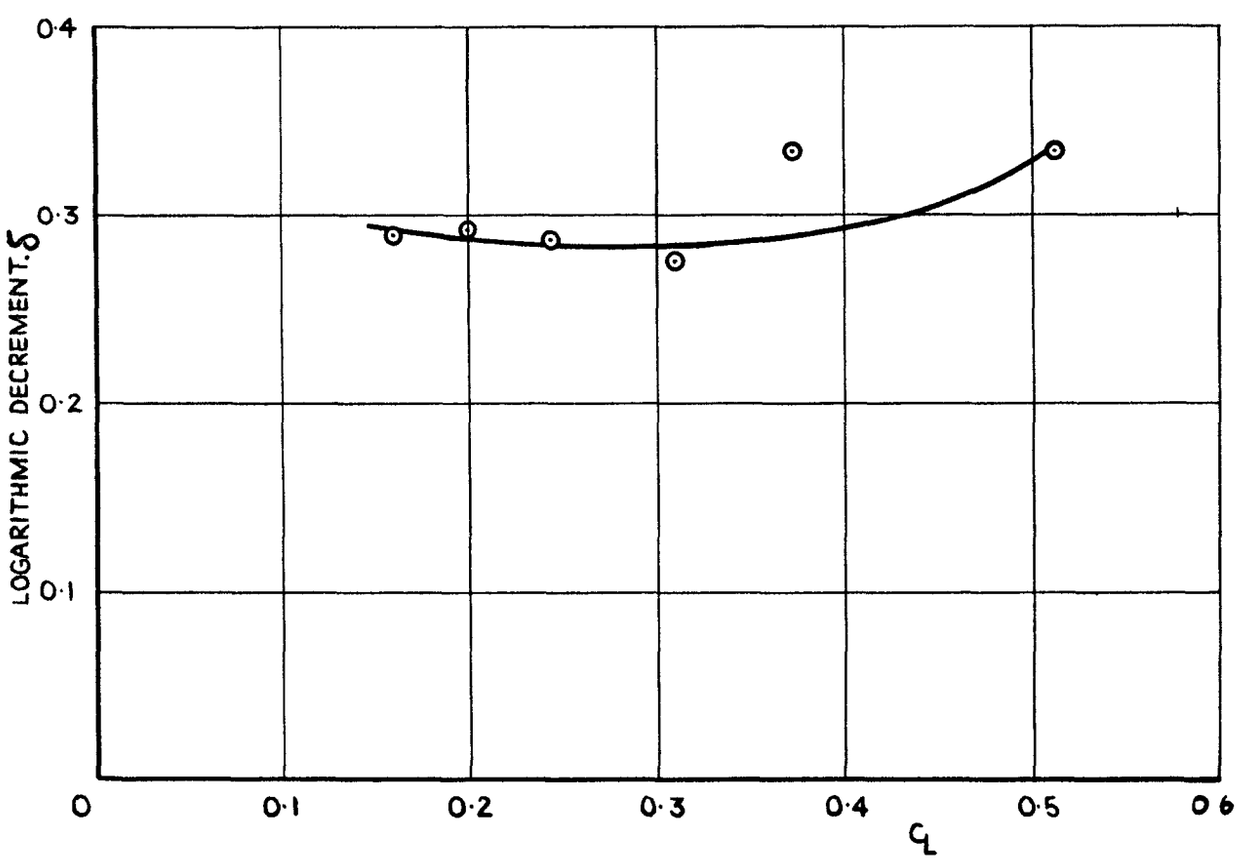

FIG. 14. DAMPING OF THE DUTCH ROLL OSCILLATION. FLAPS UP.

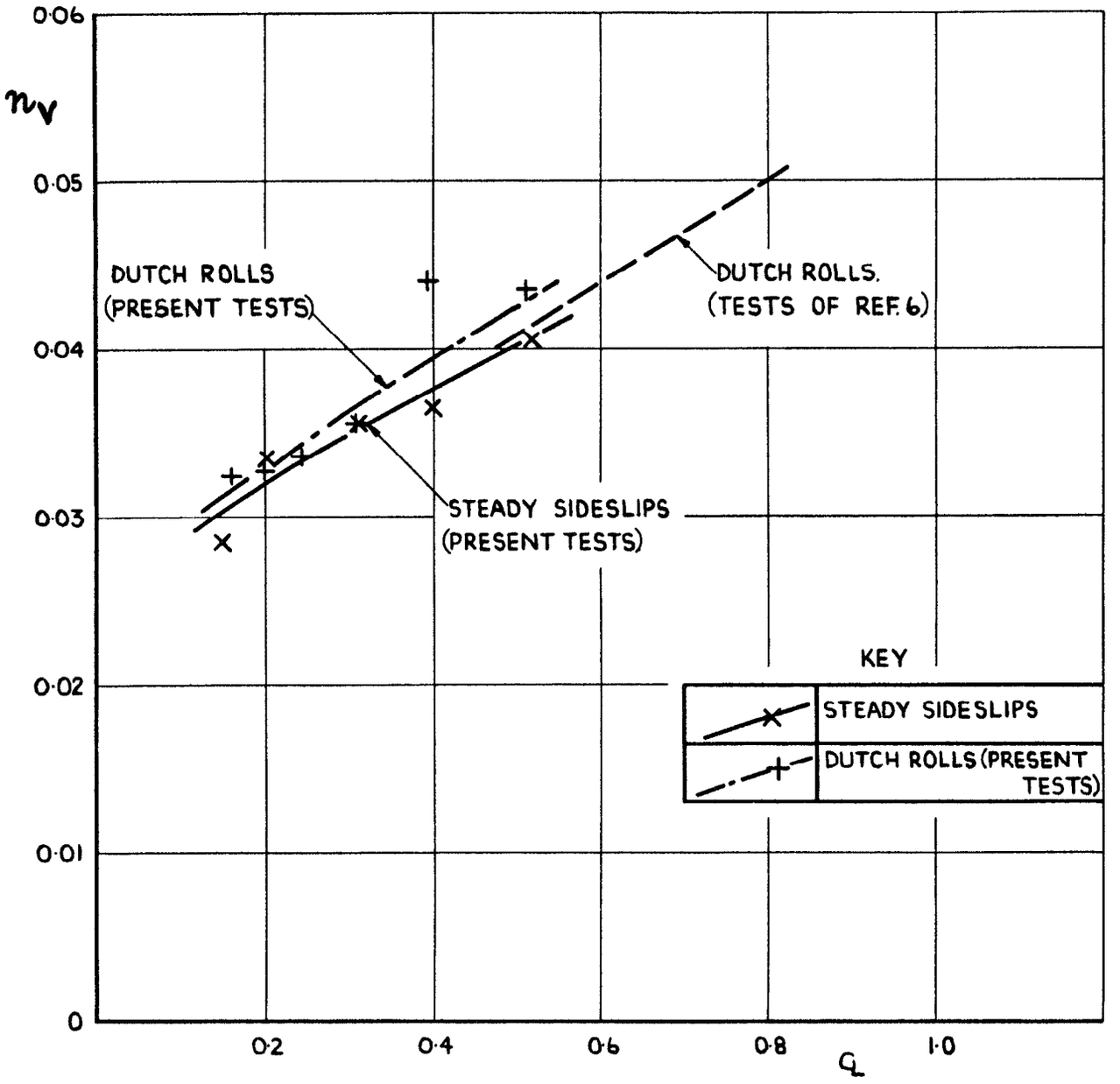

FIG. 15. DIRECTIONAL STABILITY. VARIATION OF n_V WITH C_L.

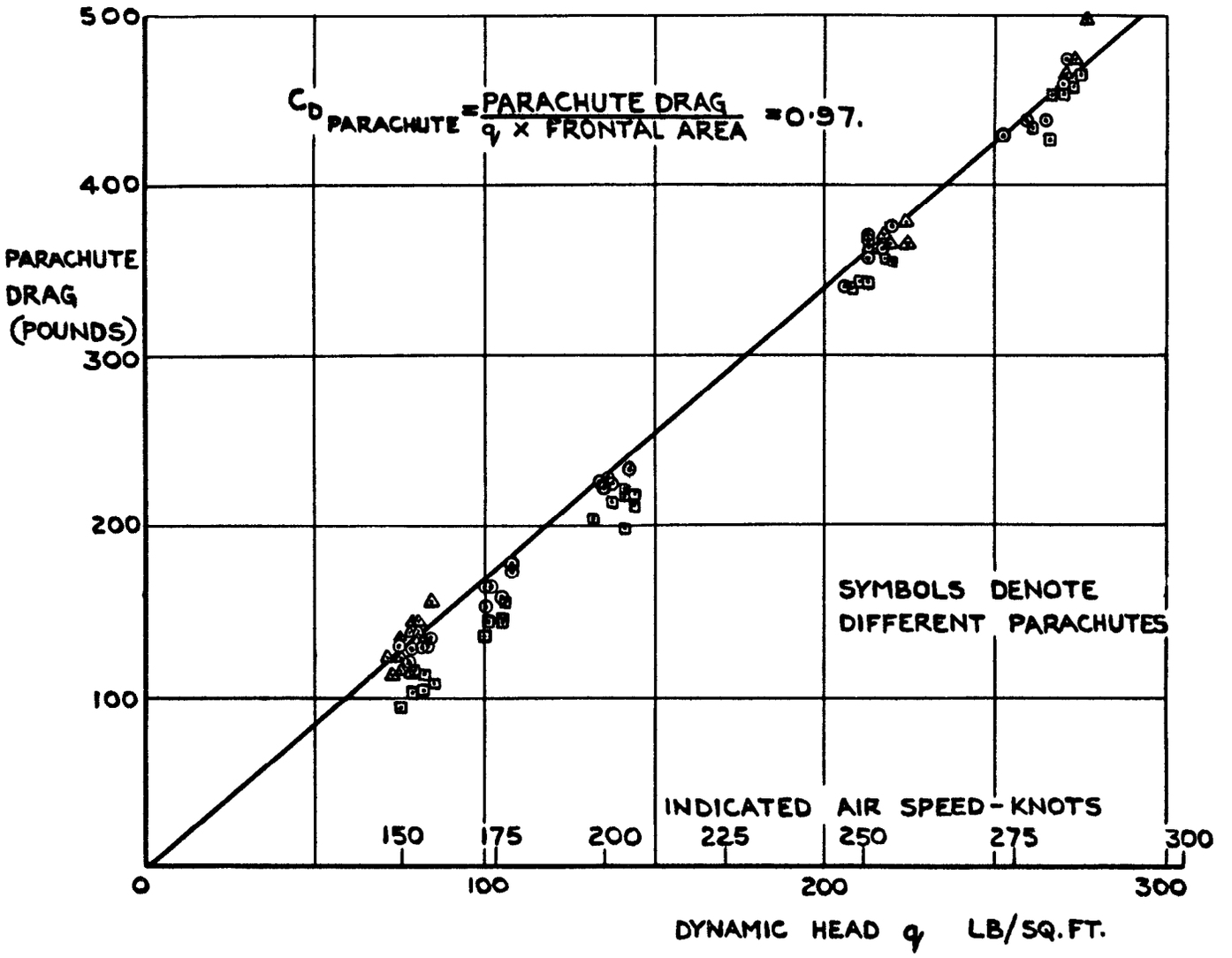

FIG. 16. MEASURED DRAG OF 18" DIAMETER PARACHUTES USED IN TESTS.

A.R.C. C.P. No.658

A.I.(42) D.H.Venom N.F.3 :
533.666.2 :
533.6.013.415/417

PROVING TESTS OF A WINGTIP PARACHUTE INSTALLATION ON A VENOM AIRCRAFT, WITH SOME MEASUREMENTS OF DIRECTIONAL STABILITY AND RUDDER POWER. Dee, F. W. June, 1962.

A trial installation of a wingtip parachute has been made on a De Havilland Venom N.F.3 aircraft to check its safety and performance before use on the Fairey Delta 2. The opportunity was also taken to measure the rudder power and the directional stability derivative n_v, of the Venom.

The arrangements for streaming and jettisoning the parachute proved safe and satisfactory. The values of the directional stability derivative measured by the parachute method agreed well with values from Dutch roll tests, also made on this aircraft.

A.R.C. C.P. No.658

A.I.(42) D.H.Venom N.F.3 :
533.666.2 :
533.6.013.415/417

PROVING TESTS OF A WINGTIP PARACHUTE INSTALLATION ON A VENOM AIRCRAFT, WITH SOME MEASUREMENTS OF DIRECTIONAL STABILITY AND RUDDER POWER. Dee, F. W. June, 1962.

A trial installation of a wingtip parachute has been made on a De Havilland Venom N.F.3 aircraft to check its safety and performance before use on the Fairey Delta 2. The opportunity was also taken to measure the rudder power and the directional stability derivative n_v, of the Venom.

The arrangements for streaming and jettisoning the parachute proved safe and satisfactory. The values of the directional stability derivative measured by the parachute method agreed well with values from Dutch roll tests, also made on this aircraft.

A.R.C. C.P. No.658

A.I.(42) D.H.Venom N.F.3 :
533.666.2 :
533.6.013.415/417

PROVING TESTS OF A WINGTIP PARACHUTE INSTALLATION ON A VENOM AIRCRAFT, WITH SOME MEASUREMENTS OF DIRECTIONAL STABILITY AND RUDDER POWER. Dee, F. W. June, 1962.

A trial installation of a wingtip parachute has been made on a De Havilland Venom N.F.3 aircraft to check its safety and performance before use on the Fairey Delta 2. The opportunity was also taken to measure the rudder power and the directional stability derivative n_v, of the Venom.

The arrangements for streaming and jettisoning the parachute proved safe and satisfactory. The values of the directional stability derivative measured by the parachute method agreed well with values from Dutch roll tests, also made on this aircraft.

UNCLASSIFIED

Published by
HER MAJESTY'S STATIONERY OFFICE
To be purchased from
York House, Kingsway, London w.c.2
423 Oxford Street, London w.1
13A Castle Street, Edinburgh 2
109 St. Mary Street, Cardiff
39 King Street, Manchester 2
50 Fairfax Street, Bristol 1
35 Smallbrook, Ringway, Birmingham 5
80 Chichester Street, Belfast 1
or through any bookseller

S.O. CODE No. 23-9013-58